Transformer oil based hexylamine-multiwalled carbon nanotubes coolant with optimized electrical, thermal and rheological enhancements

Ahmad Amiri [1,*], S. N. Kazi [1,‡], Mehdi Shanbedi [2,†], Mohd Nashrul Mohd Zubir[1], Hooman Yarmand[1], B.T. Chew[1]

[1] Department of Mechanical Engineering, University of Malaya, Kuala Lumpur, Malaysia

[2] Department of Chemical Engineering, Faculty of Engineering, Ferdowsi University of Mashhad, Mashhad, Iran

Corresponding Author: *ahm.amiri@gmail.com **(A. Amiri)**

†salimnewaz@um.edu.my **(S. N. Kazi)**

‡mehdi.shanbedi@stu-mail.um.ac.ir **(M. Shanbedi)**

Abstract

In one-pot microwave-assisted method, multi-walled carbon nanotubes (MWNT) are functionalized with hexylamine (HA). Based on the results of FT-IR, TGA-DTG, Raman, EDS, CHNS/O and TEM confirmed the functionalization of MWNT with HA. The effect of microwave-assisted functionalized MWNT with HA charged transformer oil at different concentrations are experimentally investigated for the electrical, thermal and rheological properties. According to the results breakdown voltage, flash point, density, electrical conductivity, thermal parameters, and viscosity of the synthesized transformer oil-based coolants could be an appropriate alternative for different transformers operating at the nominal voltage less than 170.

Keywords: Microwave, carbon nanotube, Electrical, Rheological, Transformer Oil, nanofluid, Breakdown

1. Introduction

Different common oils such as engine oil, transformer oil (TO), turbine oil etc. illustrate weak thermal property, so many of their applications cannot be entirely realized[1, 2]. In order to synthesize TO with good voltage insulation and power apparatus cooling and/or to increase the thermal and dielectric properties as well, numerous researchers have employed different kinds of methods. It is well known that TO can be considered as a dielectric liquid with both insulating and coolant properties. As mentioned above, the low thermal conductivity of TO play a key role in decreasing the transformer performance[3].

In the field of transformer technology, the higher thermal conductivity of TO means the higher heat transfer rate and smaller equipment size, implying more lifetime and performance[2]. In order to reach the abovementioned purpose, the innovative idea was to improve the dielectric coolants [4]. These type of fluids are synthesized via adding different nanostructures to TO, with the aim of increasing insulating and thermal properties of oil[4]. A number of studies demonstrated that about 5% growth in the thermal conductivity of TO can result a considerable cost saving to the electrical power generation and transmission distribution infrastructure[5]. Despite the idea about the fluids including solid particles with higher thermal conductivities than base fluids was reported a century years ago, the innovative concept for synthesizing coolants was introduced by Dr. Choi and his team in 1995[6].

Recently, researchers have studied the performance of transformer oil-based coolant nanofluids of different nanoparticles such as magnetite nanoparticles, Al_2O_3[7-9]. The results commonly suggested that a nanoparticle-based transformer oil coolant can be utilized to increase the cooling of a power transformer's core. It is obvious that the thermal conductivity of nanostructures may play an important role in the suspension's thermal conductivity. In the field of coolants, the higher extent of thermal conductivity of nanoparticles means the higher thermal conductivity of coolants as well as the higher heat transfer coefficient[10-12].

Among different nanostructures, carbon nanotubes (CNT) with unique thermo-physical, electrical, and mechanical properties can be selected as the promising materials[13-16]. On the other hand, various applications of CNT cannot be fully realized due to weak dispersion in solvents and feeble interaction with other materials, which resulted from strong intertube van der Waals interactions[17, 18]. To increase the interactivity of CNTs, surface functionalization was suggested as an efficient and common approach. Therefore, different functionalities such as carboxylic groups[2, 19], aminoacids [17, 20, 21] etc. have used for various applications. Arvind et al. [19] functionalized CNT with carboxylic groups to enhance the water dispersibility. Also, Zeinali et al.[2] experimentally investigated the effects of carboxylated CNT on TO. Eight effective parameters were investigated and their results reported a drop in the Breakdown voltage of TO when the carboxylated CNT was applied[2].

It is obvious that acidity of transformer oil is a destructive property. According to the previous study[6], the acidity of TO increases with the increase of water content in the oil and it becomes more soluble to the oil, which ultimately deteriorates the insulation property [22, 23]. So, despite use of carboxylic groups on CNT surface it also be used to increase despersibility in different media, thus it cannot be a good choice for TO as an additive. In order to realize an excellent dispersion of CNT in different media, a plethora number of carboxylic groups must be decorated on the surface of CNT [24]. This process first makes numerous defects on the CNT surface and then destroys the main structure and promising properties with the shortening of their lengths [24].

Choi et al. [25] synthesized and investigated the dispersions of Al_2O_3 and AlN nanoparticles in TO with surfactant of oleic acid. In order to synthesize a new kind of transformer oil-based coolant, they applied ceramic nanoparticles to enhance thermal conductivity of TO and electric insulation property. An 8% improvement in thermal conductivity and 20% in overall heat transfer coefficient were observed at AlN volume concentration of 0.5%. In addition, the viscosity of transformer oil-based coolant plays a key role in the performance of other required instruments such as pump and it has a direct connection with required power through the cooling systems.

Chen et al. [26] studied the influence of different basefluids such as silicone oil, glycerol, and water and they observed Newtonian behavior at various nano particle concentrations and temperatures. Ahmadi et al. [27] investigated the influence of CNT on engine oils coolant and their viscosities at various concentrations. They observed about 13% and 3.3% increases in the flash point and pour point of coolants from 0.1 weight% of CNT over base oil.

In the current study, multi-walled carbon nanotubes (MWNT) were first functionalized with hexylamine (HA) in a one-pot by applying green procedure under microwave irradiation. In order to realize good dispersibility in TO, decrease of defects and removal of the acidity property of TO, the proposed method have no acid treatment phase, which is the general step of previous studies. Functionalization phase was investigated via different characterization methods. In the application phase, the HA functionalized MWNT (MWNT-HA) was added to the basefluid and its properties such as , breakdown voltages, density, flash point, pour point, and transformer performance were investigated at two weight concentrations.

2. Experimental Section

2.1. Materials

The pristine MWNTs of diameter lower than 30 nm, length 5–15 μm and purity more than 95% were prepared from Shenzhen Nano-Tech Port Co. Pristine MWNT has the properties of low electrical conductivity and suitable thermal conductivity, which could be selected as one of the best choice for considering in this study as per information obtained from relevant companies. All the chemical materials of analytical grade such as methanol, $NaNO_2$, N, N-dimethylformamide (DMF), and H_2SO_4 were obtained from Merck Inc. In addition, Hexylamine (HA) was purchased from Sigma-Aldrich Co. Also, the mineral TO was obtained from Nynax, Stockholm, Sweden.

2.2. Functionalization of MWNT and preparation of Coolant

Functionalization of MWNT with diamine groups as an innovative method was reported by the present researchers [30] and Ellison et al. [28, 29]. Furthermore, Bahr et al.[30] and Price et al[31] have applied $NaNO_2$ for preparing a semi-stable diazonium ion, which has resulted a radical reaction with CNTs. Accordingly, the above-mentioned method with slight modification and under microwave irradiation was applied for functionalization of MWNT with HA. Pristine MWNT (200 mg), HA (20 ml) and $NaNO_2$ (200 mg) were poured into a vessel and sonicated for 2 hours at 50 ˚C to form a uniform suspension. About 0.5 ml of H_2SO_4 was simultaneously added drop by drop into the abovementioned suspension to accomplish the diazonium reaction. The suspension was then transferred into a Teflon vessel and was exposed to microwave radiation for 30 min at 120 °C and 700W power. The solution was cooled at room temperature, centrifuged with THF and methanol, and easily washed by vacuum filtration with a PTFE membrane. After washing several times with DMF, THF and methanol and removing any unreacted materials by checking the PH of filtrate, it was vacuum-dried for 48 h at 40 ◦C.

To synthesize MWNT-HA based transformer oil coolant of different weight concentrations, the HA treated MWNT (MWNT-HA) needs to sonicate with the known amounts of TO for 30 min. Due to the good dispersibility of HA in oil phase, the MWNT-HA could achieve an appropriate dispersion in TO media. The easily-miscible hexylamine molecules are responsible for better dispersion of MWNT-HA. The synthesized transformer oil-based coolants of different weight concentrations, such as 0.001% and 0.005% were prepared. Some essential properties of TO such as viscosity, density, flash point, pour point, breakdown voltage, electrical conductivity, and thermal conductivity are shown in Table S_1 (Supplementary information).

2.3. Experimental Apparatus

A schematic diagram of the heat transfer apparatus is shown in Figure 1. Experimental transformer was planned and constructed based on an actual transformer. There is a good combination between the size and materials of the experimental set-up and the oil-25 KVA transformer[2]. The experimental transformer was oil based including a reservoir with the dimensions of 203 *100 *221 mm^3.

A wire cylindrical heating element was employed to heat the oil and coolants. 4 PT-100 thermocouples with the accuracy of ±0.1 °C were installed in the reservoir of fluid to measure the fluid temperatures as the average temperature of them. Moreover, four thermocouples were fixed at 4 different sides of the transformer's wall to calculate the average temperature of walls as the wall temperature. Meanwhile, at an actual distance of 5 cm of the bigger wall, a 55 W blower was employed vertically to cool the big wall and introduce forced convection heat transfer.

The ammeter, thermocouples, and the voltmeter had the highest precisions of 0.001 A, 0.1 °C, and 0.1 V, respectively. The uncertainty of the experiments were calculated by Holman method [32] and the maximum uncertainty in calculating the heat transfer coefficient and Nusselt number were less than 2.1 and 5.4%, respectively.

Raman spectroscopy (Renishaw confocal spectrometer at 514 nm), thermogravimetric analysis, TGA, (TGA-167 50 Shimadzu), and transmission electron microscopy, TEM, (HT7700, High-Contrast/High-Resolution Digital TEM) were employed to analyze samples. Regarding TGA, the mass loss of samples was measured at the heating rate of 10 °C/min in air. The preparation of TEM samples comprised of several steps, such as the sonication of MWNT in ethanol, dropping the sample on a lacey carbon grid followed by drying in vacuum environment. Electrical conductivity of samples was measured by electrical conductivity meter by using two coaxial electrodes, which are the inner electrode and outer electrode. To conduct the measurement, a specific amount of sample was injected between the two electrodes. When the voltage (V) was applied to the electrodes, there would be a current (I) flowing through the sample. Then, the electrical conductivity of the sample is measured by Eq (1) [33].

$$\sigma = \frac{I}{V} * \frac{L}{S} \tag{1}$$

Where, σ, L and S are the electrical conductivity, spacing between the electrodes and the effective area of the electrodes respectively.

2.4. Data Processing

In order to investigate the influence of MWNT-HA on the thermal properties of TO in a transformer, natural & forced heat transfer coefficient (h), Nusselt number (Nu), Breakdown voltage, flash point, pour point, density, electrical and thermal conductivities and viscosity should be studied as the key parameters.

Parameters (h & Nu) were obtained from equations (2) to (4):

First, the rate of input power was calculated by Eq (2).

$$Q = VI \tag{2}$$

Here, it is obvious that thermal energy transfer between the hot wall and the cold walls. Thus, the average heat transfer coefficient (h) is determined by the equation (3).

$$h = Q/A(T_h - T_c) \tag{3}$$

Where, Q, T_c and T_h were heat flux, wall temperature and fluid bulk temperature respectively. Meanwhile, A is heat transfer area which was considered as 0.13 m^2. T_c and T_h were considered as the average temperatures obtained from the thermocouples placed on the inner body of the chamber.

The amount of Nu can be calculated from equation (4).

$$Nu = h.L/k \quad \textbf{(4)}$$

Where, L (0.05 m) is the distance between the cold and hot walls. Also, k is the thermal conductivity of MWNT-HA/TO coolants at the specific temperature and concentration.

Meanwhile, the Breakdown voltage, flash point, pours point, density, electrical conductivity, thermal conductivity and viscosity were obtained experimentally. Brookfield LVDV-III rheometer was employed to measure the amounts of viscosity. A KD_2 thermal analyzer (Decagon Devices, Inc., USA) was applied to determine the thermal conductivity of coolants and TO at various temperatures. Also, the thermal conductivity reported in this study is the average of 4 replicated measurements with the error value less than 0.0016.

3. Results and Discussion

3.1. Functionality

In order to attain one-pot and rapid functionalization method, less defective structure and selecting functional groups without acidity property, the microwave procedure based on a radical diazonium reaction was applied. Based on recent studies by the present authors[34], the mentioned radical diazonium ions was a semi-stable form, which easily reacts with MWNT. Since HA has no acidity property, there was no change in the acidity of TO after addition of MWNT-HA. In addition, functionalization process was confirmed by some characterization instruments such as derivative thermogravimetric (DTG), Raman and FT-IR spectroscopy, and transmission electron microscopy (TEM).

As discussed above, the covalent functionalization has been performed by the formation of a semi-stable diazonium ion which initiated a radical reaction between the nanotubes and HA chains. FT-IR spectroscopy has been employed as one of the best evidences, which is illustrated in Figure 2 panel (a). In contrast to the pristine sample, the FT-IR spectrum of the MWNT-HA demonstrates a couple of peaks at the ranges of 2850–3000 cm^{-1}, indicating the presence of C-H stretching vibrations[35]. Also, the peaks at 1396 cm^{-1} and 1460 cm^{-1}, arise from the bending vibration of the CH_2 group [35]. Formation of abovementioned peaks after functionalization along with the lack of amine peaks can depict the diazonium reaction between MWNT and HA[29, 34]. More importantly, the peak at 1492 cm^{-1} was associated with the stretching vibrations of C=C, which is due to disruption of aromatic π-electrons on the MWNT surface.

Raman characterization is a strong measurement for analyzing structure, sp^2 and sp^3 hybridized carbon atoms in carbon-based materials and functionalization by following alterations in hole [36-39]. The Raman spectra of the pristine MWNT, and MWNT-HA are presented in Figure 2 panel (b). While the pristine MWNT is weak in terms of D intensity, the fairly strong D band in the MWNT-HA sample can be seen at 1343 cm^{-1}.

The ratio of the intensities of the D-band to that of the G-band (I_D/I_G) was considered to be the amount of disordered carbon (sp^3-hybridized carbon) relative to graphitic carbon (sp^2-hybridized carbon)[39]. In functionalization studies of MWNT, the higher intensity ratio of I_D/I_G indicates the higher disruption of aromatic π-π electrons, implying partial damage of the graphitic carbon produced by covalent functionalization [39, 40]. The I_D/I_G ratio of MWNT-HA (0.91) is relatively higher than that of pristine MWNT (0.49), which confirmed the successful functionalization via a diazonium reaction under microwave irradiation. A significant increase in I_D/I_G can also confirm that the present method is completely successful for functionalization of MWNT without acid-treatment phase.

As a further evidence, the thermogravimetric analysis (TGA) was applied to investigate functionalization of MWNT with HA. TGA is a technique of thermal analysis in which alterations in structure of materials are measured as a function of temperature. Also, TGA obviously present results about chemical functionalization of MWNT with different groups[41, 42].

Figure 2 panel (c) presents the TGA and derivative thermogravimetric (DTG) curves of the pristine MWNT and MWNT-HA. It can be seen that the TGA result of pristine sample illustrates no mass loss up to 500 °C. However, there is an obvious weight loss in the temperature range of 50–150°C in the HA-MWNT curve. This mass loss was attributed to the functionality of HA as an unstable organic part on the surface of MWNT. Also, it is obvious that DTG curve of the pristine MWNT shows no phase of degradation up to 500 °C and a noticeable step of mass loss in the temperature range of 500–730 °C is attributed to the bulk degradation temperatures of the main graphitic structures. In addition to the first step of mass loss, the first step of degradation with DTG curve of MWNT-HA at the temperature range of 50–150 °C is associated with the bulk degradation temperatures of HA as an unstable organic loaded on the surface of MWNT.

The degree of functionalization of modified MWNT is generally calculated by means of thermogravimetric analysis (TGA). Functionalization degree of MWNT-HA was calculated in order to assess the functionalization yield of the proposed method. The following formula is used to measure the functionalization degree from TGA results[43]:

$$\text{Degree of Functionalization} = \frac{\text{Weight loss of attached function (gr)} * \frac{1000\text{mmol}}{\text{Molecular weight of attached function}}}{\text{MWNT weight loss}}$$

While pristine MWNT lost only 1.01% of mass up to 500 C, TGA curve of the HA-functionalized MWNT display a considerable mass loss of 11.1% in the range of 50–200 °C corresponding to the decomposition of the attached HA moiety. On the basis of TGA weight loss, we estimated that the amount of functional groups per gram (mmol/g) of MWNT-HA is 1.4661.

Overall, TGA or DTG, FT-IR and Raman results are in good agreement with each other on functionalization of MWNT with HA. Utilizing microwave method and semi-stable diazonium ions simultaneously provided a very effective route to attack the main graphitic structures of MWNT.

3.2. Morphological analysis

TEM analysis was carried out to study the morphological structure of MWNT. Figure 2 panels (d, e and f) shows the TEM images of the MWNT-HA. As a first cue of functionalization, there are some MWNT with open tips, which is resulted by radical reaction of diazonium ion with MWNT. In addition, the functionalization procedure alters the graphitic (sp^2) carbon network to sp^3 hybridized states of carbon, which is in a good agreement with more defects on the MWNT surface after treatment. Thus, more surface roughness in the MWNT-HA images is logical. Even though TEM images illustrate no cue of functional groups, the more surface deterioration of treated MWNT with HA can be considered as one of the main evidence[13]. These morphological changes are in agreement with the DTG, FT-IR, and Raman results.

3.3. Elemental Analysis

To confirm the diazonium coupling, elemental analyses were performed by the energy dispersive X-ray spectroscopy (EDS) and combustible elemental analysis (CHNS/O). EDS spectra of pristine MWNT and MWNT-HA (Figure 3) show a trace amount of Ni, O and Cd in their chemical structures. The trace amount of Cd and Ni are mainly due to the trapped catalysts during pure MWNTs' synthesizing. EDS results are presented in Table 1 to ascertain accurately the exact amount of each elemen. EDS analysis shows the increase of oxygen content and the presence of a very little amount of nitrogen in the MWNT-HA. Note that the MWNT-HA showed high purity except a very small amount of nitrogen and oxygen. It is noteworthy that our attached functional group has just C and H elements. To confirm the results obtained by EDS and to obtain information on the hydrogen content, combustible elemental analysis was performed. Combustible elemental analysis (CHNS/O) was performed using a Perkin Elmer 2400 series II and was used to measure carbon, oxygen, nitrogen, and hydrogen elemental content. The instrument was used in CHN operating mode to convert the sample elements to simple gases (CO_2, H_2O and N_2). The PE 2400 analyzer automatically performed combustion, reduction, homogenization of product gases, separation and detection. The results for CHNS/O analyzer are shown in Table 2. The results were in very good agreement with those obtained by the EDS results. As more evidence, CHNS/O results show that H content substantially increase in MWNT-HA, which further confirms that hexane has been successfully grafted onto MWNT. Also, no trace of nitrogen was observed in the MWNT-HA, which confirm a successful diazonium coupling.

Table 1. EDS results for pristine MWNT and MWNT-HA.

Element Symbol	**Pristine MWNT**	**MWNT-HA**
C	93.1±0.7	90.2±0.9

O	2.9±1.1	3.2±0.5
N	0.0	0.1±0.9

Table 2. Elemental composition of Pristine MWNT and MWNT-HA.

Sample	**Chemical composition (wt. %)**			
	C	N	O	H
Pristine MWNT	90.23	0.00	2.54	1.09
MWNT-HA	89.85	0.09	2.41	3.28

3.4. Stability analysis

Figure 4 panel (a) illustrates the UV–vis spectra of the MWNT for weight concentrations of 0.001 and 0.005. UV–Vis spectroscopy is commonly applied for the investigation of the stability of coolant including solid nanoparticles and is able to measure the sedimentation time. According to the Beer–Lambert's law, the absorbance of a solution is directly proportional to the concentration of the absorbing species such as particles in the solution. As a raw spectrum of MWNT-HA/TO coolant, sharp peak at 275 nm is attributed to the presence of MWNT, and intensity of peak increases with weight concentration. Quantitative analysis of the dispersion state and the long-term stability of the MWNT and MWNT-HA/TO coolants were performed in UV–Vis spectroscopy, as shown in Figure 4 panel (b). Thus, the absorbance at the wavelength of 275 nm was measured during 30 days for both weight concentrations. It can be seen that the relative concentration of MWNT-HA decrease insignificantly over time. As a result, the maximum sediment of 26.1% was obtained for highest weight concentration of 0.005, which confirmed the suitable dispersibility of MWNT-HA in TO. To check whether the decrease in signal intensity by time is just due to reversible particle settling or gradual irreversible particle aggregation, Figure 4 panel (c) is plotted. The UV–vis spectrum of the MWNT-HA for weight concentrations of 0.001 and 0.005 obtained by performing UV measurements for 30 days on suspensions mechanically shaken every day. The sonication were performed for 5 min at room temperature with power rating of 390 W. The measurement was again carried out at peak wavelength of each material to trace the alteration in the intensity which can be further used to describe the suspension stability at both weight fraction of 0.001% and 0.005%. It can be seen that both colloidal mixtures show lower than 1% decrease in the relative concentration as the time progressed, indicating that the colloidal suspensions have been remained stable for 1 months without irreversible particle aggregation.

Also, the particle size distribution change is analyzed using the dynamic light scattering (DLS) method to check the aggregate size with time. To measure DLS, the samples were transferred into the folded capillary cell (polycarbonate with gold plated electrodes) for investigation of particle size distribution using Zetasizer Nano (Malvern Instruments Ltd., United Kingdom) at 25 ^{0}C.

Figure 5 is the graphs of the particle size distributions in the nanofluids measured by the DLS method. These graphs present the size distribution of the particles. Figure 5 panels (a-f) show the DLS results of MWNT-HA. Although the difference is insignificant, the overall distribution exhibits that the distribution is found to move to the a bit larger particle size when the distribution of the final day is compared with those of other days, i.e., the particles are insignificantly aggregated. Also, a comparison of particle size distribution of pristine MWNT (Figure 5g) and MWNT-HA (Figure 5a-f) represented a big difference. While pristine MWNT was completely degraded after 24 hr to reach particle size distribution of 3033 nm, the MWNT-HA materials have been showing the particle size distribution around 400 nm for 35 day, indicating stable colloidal system of them in TO media. Therefore, the existence of MWNT-HA in TO provides a great benefit, MWNT-HA provides a stable colloidal system, which can enhance the heat transfer properties.

Table 3 demonstrates the particle size distributions and zeta potential for pristine MWNT/TO and MWNT-HA/TO colloids over a period of 35 days. First, MWNT-HA/TO shows no big aggregation and coagulation at both concentrations. It can be seen that the particle size distribution for MWNT-HA/TO nanofluids shows a gradual increase in the overall hydrodynamic size, which substantiates the formation of small aggregation, which is in agreement with UV-vis results. On the other hand, pristine MWNT was mostly settled after 24 hr. The above results confirm the critical role of HA molecules which act as covalent stabilizer to prevent rapid colloidal instability associated with the increase in graphitic domain within the carbon-based structure.

According to the stabilization theory, the electrostatic repulsions between the particles increase if zeta potential has a high absolute value which then leads to a good stability of the suspensions. Particles with a high surface charge tend not to agglomerate, since contact is opposed. Typically accepted zeta-potential values are summarized in Table S_2[44].

Table 3 is also shown the zeta-potential and the polydispersity index (PDI) for pristine MWNT and MWNT-HA/TO at their natural PH. The zeta-potential and polydispersity index (PDI) are commonly utilized as an index of the magnitude of electrostatic interaction between colloidal particles and thus can be considered as a measure of the colloidal stability of the solution. According to the Table S_2, zeta potential must be as large as possible (positively or negatively) to make a common repulsive force between the particles [45]. It can be seen that after functionalization with HA, MWNT-HA shows a more negatively charged and is around -45 mV over a period of 35 days. The zeta potential results of MWNT-HA in TO media suggest an appropriate stability over a period of 35 days at 25 ° C. Indeed, the zeta-potential gradually show some fluctuations over a period of 35 days, in spite of remaining mostly stable with time [45].

Table 3. Zeta potential, average particle size distribution, mobility and polydispersity Index (PDI) of pristine MWNT and MWNT-HA in TO media.

Label in Figure	Sample	Time (day)	Average particle size distributions (nm)	Polydispersity Index(PDI)	Zeta Potential(mV)	Mobility(μmcm/Vs)
a	MWNT-HA	1	367.4	0.297	-52.3	-4.097
b	MWNT-HA	7	407.3	0.222	-49.4	-3.870
c	MWNT-HA	14	401.5	0.259	-46.9	-3.678
d	MWNT-HA	21	411.0	0.239	-38.6	-3.024
e	MWNT-HA	28	400.9	0.245	-46.6	-3.655
f	MWNT-HA	35	389.3	0.251	-50.4	-3.951
g	Pristine MWNT	1	3033	0.655	-23.6	-1.853

3.5. Electrical and Thermo-physical analysis

3.5.1. Electrical properties

As a key parameter, the electrical resistivity of MWNT-HA/TO coolants as well as pure TO was investigated in the temperature range of 20–50 °C. Electrical conductivity and resistivity behaviors of samples for different weight concentrations were illustrated in Figure 6 panels (a) and (b), respectively. The results of electrical conductivity and resistivity of the pure TO and synthesized coolants demonstrated different changes by MWNT-HA loading into the pure TO. Alteration of the electrical conductivity and resistivity was in the range of 7-23% with changing concentration. It can be seen that the prepared samples present larger electrical conductivity enhancement at higher weight concentration of MWNT-HA. Thus, the intrinsic electrical transfer capacity of the MWNT should be the main reason for electrical conductivity enhancement or decreasing thermal resistance. Also, the lack of acidic agent retards the corrosion phenomenon and enhance the electrical conductivity of the prepared coolants, which as a result increases the lifetime of the system.

3.5.2. Thermal conductivity

Obviously, TO can be considered as the oil with a high electrical insulation property and heat transfer agent. It is obvious that TO with higher thermal conductivity can be more useful. Similar to other critical factors, the thermal conductivity and the rate of heat transfer of TO play a key role in the selection of the transformer fluid. By looking at the transformer oil's normal operating temperature (253 K to 363 K), the effect of temperature on the thermal conductivity of TO also plays a key role in the performance of transformers[46]. In contrast to other basefluids, the thermal conductivity of transformer oil decreases with increasing temperature[46]. It is a big disadvantage in applying transformer oil, in particular, at high range of temperature, resulting in lower performance of transformer[2]. Note that the extent of thermal conductivity's reduction with temperature increasing is different for different transformer oils. Decrease of molecular association with temperature increasing makes a considerable difference to TO's thermal conductivity because the molecular chain is so long and the molecular weight is so great. Thus, it is obvious that TO with higher thermal conductivity can be more useful. The previous studies illustrated that various parameters such as thermal conductivity of working fluid and nanostructures, size, concentration, temperature, PH and shape of nanostructure influence the thermal conductivity of coolants[47, 48]. Also, some of the thermal phenomena such as Brownian motion, thermophoresis, and diffusiophoresis can influence the thermal conductivity of coolants[2, 49].

Figure 7 the thermal conductivity plot of MWNT-HA/TO coolant as a function of temperature and concentration. Two different weight concentrations of 0.001% and 0.005% are considered and the variation of thermal conductivity with concentration and temperature are studied. To avoid significant increase in effective viscosity and electrical behaviors, MWNT-HA at low concentrations is considered in the present study. Figure 7 obviously demonstrates that the thermal conductivity of MWNT-HA/TO coolant is higher than that of pure TO. Also, it can be seen that the thermal conductivity of the TO decreases as the temperature increases, where the MWNT-HA/TO coolants at both concentrations show the upward trends. In similar study, Zeinali et al.[9] Showed that the thermal conductivity of MWNT-COOH/TO coolants increased up to 60 °C and it decreased considerably at higher temperature. This drop may be attributed to the settlement of MWNT, which can be resulted from the disruption of carboxyl groups on the MWNT surface at high temperature. In contrast with previous study[10], the problem of accumulation at 60°C is completely eradicated by the functionalization of MWNT with HA. On the other hand, some researchers in the field of heat transfer concluded that the nanoparticles are governed by the continuous irregular reciprocating motion and phenomena such as Brownian motion, thermophoresis and diffusiophoresis which could influence thermal conductivity of coolant [4]. Above all, it is a big success that the trend of thermal conductivity illustrates a rising trend over the temperature range of 30-80 °C.

On the other hand, the obtained results confirm that the temperature play a key role in increasing the thermal conductivity of MWNT-HA/TO coolant, which cannot be neglected. For coolants loaded with MWNT, the vital role in heat transfer enhancement is played by the nanoparticles[50, 51]. Liquid molecules generate layers around the MWNT, thereby altering the local ordering of the liquid layer at the interface region. Thus, the liquid layer at the interface would exhibit a higher thermal conductivity compared to the base-fluid. Differences in thermal conductivity enhancement may be attributable to differences of the thermal boundary resistance around the nanoparticles occurring for different base fluids [52]. The higher slope in thermal conductivity of MWNT-HA/TO coolants with higher concentration is due to higher rate of formation of the surface nanolayers [10]. In addition, the role of Brownian motion of particles in nanofluids may be an important parameter in determining the thermal conductivity enhancement and also an important factor, in particular for cases with significant change in viscosity with temperature, which is certainly the case for TO [52]. According to the recent studies[19, 53, 54], increasing the local ordering of the liquid layers at the interface region is one of the main reason for thermal conductivity enhancement. Thus, the resistance for heat removal is decreased by thinning of the thermal boundary layer via MWNT loading in basefluids and preparing nanolayers with higher thermal conductivity than the bulk liquid.

A summary of experimental studies on the thermal conductivity of TO-based nanofluids is listed in Table S_3. It is worth mentioning that most of the recent studies focused on suspensions with high nanoparticle's concentration, which increase the possibility of sediment. As compared with recent studies[2], the present work reaches higher enhancement in thermal conductivity at similar experimental condition. For example, Patel et al. [55] obtained 10, 11.5, 14 and 17% enhancements in the thermal conductivities of TO-based nanofluids by the addition of Al_2O_3 at 20, 30, 40 and 50 °C, respectively. Such enhancements are obtained for 3% Al2O3 loading, while we work at very low weight fractions of 0.001 and 0.005. In fact, the strategy of the present study is the utilization of low concentration of highly-soluble MWNT-HA in TO to avoid sediment, since the bulk fluid in the transformer is motionless.

3.5.3. Convective heat transfer coefficient

In order to investigate the convective heat transfer coefficient, several experiments at different input powers of 49.76, 60.25, 69.95, 81.1, 90.4, 100.36, 110.42, 120.6, 130.19, 140.16 and 149.83 were applied. Also, the natural and forced heat transfer coefficients were studied at both the weight concentrations of MWNT-HA at different powers.

Natural convection heat transfer is occurred by the buoyancy force, which results from the density deviations formed by temperature variations in the layers of fluid. This type of heat transfer generate in the absence of an external source for the movement of bulk fluid. According to the previous study [56], when a fluid contacts with a surface with higher temperature, the molecules of the fluid separate and form a layer of lower density. As a result, the layers of fluid with lower density are displaced by the cooler layers of fluid, thus the cooler layers of fluid sink. Noteworthy, the nanostructures concentrations and thermal conductivity can also influence natural convection in coolants [2].

The natural convection heat transfer coefficient and Nusselt number of pure TO and MWNT-HA/TO coolants versus input power are illustrated in Figure 8 panels (a) and (b), respectively. It can be seen that similar upward trends are obvious in the presence of the pure TO and MWNT-HA altered coolants in both figures. It is obvious that the heat transfer coefficient is a function of temperature. According to the results, the input power increases with the increase of the average temperature of bulk fluid in transformer, which is implying higher heat transfer coefficient. As the thermal conductivity of the coolants at different temperatures is applied for calculation, the evaluated Nusselt number results show some weak fluctuations.

Forced convection is a mechanism of heat transfer in which fluid motion is created via an external source such as fan and pump. The amount of forced convection heat transfer coefficient and Nusselt number versus input power are respectively shown in Figure 8 panels (c) and (d) for pure oil and MWNT-HA/TO coolants. Natural convection heat transfer coefficient and Nusselt number increases with the increase of input power and concentration, the forced convection heat transfer also shows similar results of enhancement with the increase of power and concentration. Surprisingly, the amount of thermal conductivity, heat transfer coefficient and/or Nusselt number show significant enhancements in the presence of MWNT-HA, which is attributed to the good dispersibility of MWNT in TO as one of the reasons.

The enhancement of convective heat transfer can be attributed to the reduction of thermal boundary layer thickness. Arvand et al. [50, 57] showed that carbon nanomaterials such as MWNT has a tendency to decrease the thermal boundary layer thickness, which lowers the difference between temperatures of bulk fluid and wall in transformer and subsequently enhances the convective heat transfer coefficient. To clarify it, heat transfer coefficient can be approximately modeled as k/δ_t, where δ_t represents the thermal boundary layer thickness. So for increasing the heat transfer coefficient, either k should be increased or δ_t should be decreased or both. As a future comparison, Table S_4 also shows a comparison of the natural convection and forced convection heat transfer coefficients of nanofluids with different nanoparticles loading. The convective heat transfer coefficient of MWNT-HA/TO nanofluid was compared with those of other nanoparticles-based TO nanofluids reported in the literature. Obviously, the present samples had a relatively high natural convection and forced convection heat transfer coefficients in comparison to other nanoparticles loading in TO at similar weight fraction, in particular, as compared with MWNT-COOH/TO nanofluids [2] at similar experimental conditions. Our results showed the natural convection and forced convection heat transfer coefficient enhancements of 23 and 28% at weight fraction of 0.005, which demonstrate a significant increase at a very low concentration.

3.5.4. Breakdown voltage

Breakdown voltage is a dielectric strength of TO and plays an essential role in the electrical performance of transformers. Breakdown voltage is obtained via detecting the voltage required for generation of spark between two electrodes with a precise gap in the oil. Small extent of breakdown voltage demonstrates the presence of moisture content in the TO. According to the previous studies [2, 58], different impurity and percentage of moisture content can easily disturb the breakdown voltage results. On the other hand, functionalization of MWNT is the only route for increasing the colloidal stability of MWNT in TO media. Thus, it is essential to apply functional groups with hydrophobic properties for functionalization of MWNT. HA as a functional group can meet both criteria's of good dispersion and hydrophobic property. In addition, to prevent acidity, one-pot and novel method without acid-treatment is employed.

Breakdown voltage of pure TO with and without sonication, MWNT-HA/TO at both weight concentration of 0.001 and 0,005 are plotted in Figure 9. Also, the mean breakdown voltage with standard deviation are listed in Table 4. In order to measure the dielectric breakdown voltage with different weight fractions of MWNT-HA in the colloidal suspension, the experiment is repeated 60 times for each of the weight concentration according to ASTM D-92 standard using the dielectric breakdown measurement device, Mugger's automatic laboratory oil tester. All experiments were performed using mushroom electrodes set at 1mm gap and at room temperature. The dielectric breakdown voltage of all samples measured 1 day after preparing. The most influential factor affecting the performance of the dielectric strength of transformer oil is the degradation caused by water and other contaminants [59], which sonication process could also introduce moisture in oil. Figure 9 panels (a) and (b) show the dielectric breakdown voltage of pure oil with and without 30 min sonication (time for performing diazonium reaction) to investigate the effect of sonication process on TO performance. Results suggest that the sonication has an insignificant effect on the dielectric breakdown voltage (~ 0.4 kV), which is obtained by doing just 30 min sonication with the Bioruptor (4 sec "ON", 4 sec. "OFF").

Figure 9 panels (c) and (d) show the experimental results with the various weight concentrations of MWNT-HA. Generally, increasing the MWNT-HA concentration leads to a mild decrease of the dielectric breakdown voltage. Again, the mean breakdown voltages and standard deviations for above-mentioned samples are given in Table 4. It was found that breakdown voltages level-off with the rising test number, no upward or downward trend was obtained in experiments, which owes to the effective energy control of the test equipment. With the increase of weight concentration of MWNT-HA in TO from 0.001 to 0.005%, the dielectric strength decreases from 54.098KV to 52.066KV. The standard deviations of both samples are larger than that of transformer oil, indicating the breakdown voltage of samples is less predictable. The MWNT-HA loading in TO media leads to a small drop in breakdown voltage, which mainly caused by MWNT.

Table 4. Breakdown voltage (kV) of the pure TO and MWNT-HA/TO at different concentrations

Samples	Mean Breakdown voltage (KV)	S.D. (KV)
Pure TO	58.03166667	1.137174

Sonicated Pure TO	57.65333333	1.311039
MWNT-HA/TO (0.001%)	54.09833333	1.60521
MWNT-HA/TO (0.005%)	52.06666667	2.47283

3.5.5. Density of fluids

The density of MWNT-HA/TO coolants as well as pure TO at various temperatures is illustrated in Figure 10. Density plays a key role in evaluating the natural convection heat transfer. As mentioned above, natural convection is a function of buoyancy force or density variation. As shown in Figure 10, there is a diverse connection between temperature and density of fluids. Also, the density of coolants increases with the increase of MWNT-HA concentrations.

3.5.6. Flash point

Flash point is considered as the temperature at which TO produces sufficient vapors for creating a flammable mixture with air. Flash point is a very essential temperature for defining the probability of fire hazard in transformer in the presence of TO. Therefore, higher flash point can be considered as a desirable property for TO[60].

A seta semi-automatic cleveland open cup flash point tester was used to measure flash point. Flash point of the pure TO with and without sonication and also MWNT-HA/TO at two different weight fractions were measured on the basis of American Society for Testing and Materials (ASTM) D-92[61]. The trend of changes of flash point as a function of MWNT-HA concentration is shown in Figure 11. First, flash point was tested for the pure oil with and without sonication to investigate the effect of sonication. Variation of flash point in the presence of sonication and lack of sonication are given in Figure 11, which show around one degree increase in the volatility of the TO with performing sonication for 30 min. Also, the variation of flash point as a function of MWNT-HA concentration is indicated an increase in the volatility of the TO with the MWNT addition. It is obvious that higher flash point temperatures is required for safer handling of TO. The rate of increase in flash point of the MWNT-HA/TO coolant at 0.001 weight fraction with respect to the TO is 4.69%, and the highest amount of increase is related to the 0.005 weigh fraction of sample, which is 7.86%.

3.5.7. Viscosity

Viscosity is known as the resistance of fluid to flow. High-resistance transformer oil produces an obstacle for the convection circulation in the transformers. Obviously, low viscosity is essential property for an excellent TO. Another critical property for TO is the decrease of viscosity with the increase of temperature at a lower rate. The viscosity of pure TO and MWNT-HA/TO coolant at different concentrations and high shear rate of 235 s^{-1} are investigated experimentally, as shown in Figure 12.

Similar to other oil-based nanofluids, the rheological behavior of MWNT-HA/TO (Figure 12a) shows two typical characteristics: (i) an enhancement of viscosity with increasing weight fraction of MWNT-HA, and (ii) a decrease in viscosity with increasing temperature, which is due to weakening of the intermolecular forces of the fluid itself. To illustrate the amount of enhancement in viscosity with MWNT-HA loading, Figure 12b is plotted. It shows the enhancement in the MWNT-HA/oil viscosity, which is less than 10 % for both weight fractions and all temperatures. It can be concluded that the enhancement in the MWNT-HA/oil viscosity is insignificant with increase in weight concentration, which can be attributed to the low weight fraction of MWNT-HA in oil. In addition, in agreement with Ko et al. [62], viscosity decreases with the increase in temperature.

Also, the viscosity of pure TO and MWNT-HA/TO coolant as a function of the shear rate for different concentrations are represented in Figure S_1 (supplementary information). The effective viscosities of pure transformer oil and treated coolants were measured for the shear rate range of 35-235 S^{-1}. First, MWNT-HA/TO and pure TO have a linear shear stress/shear rate relationship, which can be categorized as a Newtonian fluid [2, 63]. It may be seen for all temperatures, viscosity of the TO is independent of the shear strain rate, indicating Newtonian behavior. Also, after the addition of MWNT-HA, samples show the Newtonian behavior.

We believe that since TO exhibits Newtonian behavior, it dominates the rheological property and the whole mixture behaves like a Newtonian fluid with low concentrations of MWNT-HA. Due to some fluctuations and the significant error in measurement, we were not able to identify the exact amount of viscosity for shear rate around zero. Based on some recent researches[2, 63, 64], TO categorizes as the Newtonian fluids.

Conclusion

MWNT is functionalized via hexylamine (HA) along with diazonium reaction under microwave radiation in a rapid and one-pot technique to obtain highly dispersed MWNT in TO media without acidic property. The procedure was fast and simple and resulted in a suitable degree of hydrophobic functionalization as well as solubility in TO media. Based on the results of FT-IR, TGA-DTG, Raman, EDS, CHNS/O and TEM confirmed the functionalization of MWNT with HA. The results of natural and forced convection heat transfer coefficients, breakdown voltage, flash point, density, electrical and thermal conductivities and viscosity verified the synthesized MWNT-HA based transformer oil is a promising alternative oil for use in transformers. Also, the promising achievements in the thermal and rheological properties support this claim. We obtained 10% enhancement in the thermal conductivity of TO-based nanofluids at a very low weight concentration of 0.005. Also, results showed the natural convection and forced convection heat transfer coefficient enhancements of

23 and 28% at weight fraction of 0.005, which demonstrate a significant increase at a very low concentration. Observation of enhancement in natural- and forced-convection heat transfer coefficients and thermal conductivity of working fluid with MWNT-HA loading in TO, a feeble decrease in breakdown voltage and lack of remarkable change in rheological properties can be resulted in higher performance transformer.

Acknowledgment

The authors gratefully acknowledge Bright Sparks Unit of the University of Malaya, UMRG Grant RP012B-13AET and High Impact Research Grant UM.C/625/1/HIR/MOHE/ENG/45, Faculty of Engineering, University of Malaya, Malaysia for support to conduct this research work.

Nomenclature

Nu	Nusselt number
T_c	Average Temperature of walls, °C
h	Heat transfer coefficient, W/m^2 K
k	Thermal conductivity, W/m K
L	Length, m
T_h	Average Temperature of oil, °C
Q	Input power, W
A	Heat transfer area
V	Voltage, V
I	Current, A

References

1. A. Amiri, M. Shanbedi, H. Yarmand, H. K. Arzani, S. Gharehkhani, E. Montazer, R. Sadri, W. Sarsam, B. Chew and S. Kazi, *Energy Conversion and Management*, 2015, **105**, 355-367.
2. A. Beheshti, M. Shanbedi and S. Z. Heris, *J Therm Anal Calorim*, 2014, **118**, 1451-1460.
3. B. X. Du and X. L. Li, 2014.
4. C. Choi, H. S. Yoo and J. M. Oh, *Current Applied Physics*, 2008, **8**, 710-712.
5. J. Davidson and D. Bradshaw, *Journal*, 2003.
6. S. Chol, *ASME-Publications-Fed*, 1995, **231**, 99-106.
7. J. G. Hwang, M. Zahn, F. M. O'Sullivan, L. A. Pettersson, O. Hjortstam and R. Liu, *Journal of applied physics*, 2010, **107**, 014310.
8. V. Segal, A. Rabinovich, D. Nattrass, K. Raj and A. Nunes, *Journal of magnetism and magnetic materials*, 2000, **215**, 513-515.
9. T. Cader, S. Bernstein and C. Crowe, *Journal*, 1999.
10. A. Amiri, R. Sadri, M. Shanbedi, G. Ahmadi, B. Chew, S. Kazi and M. Dahari, *Energy Conversion and Management*, 2015, **92**, 322-330.
11. A. Amiri, M. Shanbedi, H. Amiri, S. Z. Heris, S. Kazi, B. Chew and H. Eshghi, *Applied Thermal Engineering*, 2014, **71**, 450-459.

12. M. Shanbedi, S. Z. Heris, A. Amiri and M. Baniadam, *Journal of Dispersion Science and Technology*, 2014, **35**, 1086-1096.
13. A. Amiri, R. Sadri, G. Ahmadi, B. Chew, S. Kazi, M. Shanbedi and M. S. Alehashem, *RSC Advances*, 2015, **5**, 35425-35434.
14. M. Shanbedi, D. Jafari, A. Amiri, S. Z. Heris and M. Baniadam, *Heat and Mass Transfer*, 2013, **49**, 65-73.
15. M. N. M. Zubir, A. Badarudin, S. Kazi, M. Misran, A. Amiri, R. Sadri and S. Khalid, *Journal of Colloid and Interface Science*, 2015.
16. J. Saien, H. Bamdadi and S. Daliri, *Journal of Industrial and Engineering Chemistry*, 2015, **21**, 1152-1159.
17. B. Ghiadi, M. Baniadam, M. Maghrebi and A. Amiri, *Russian Journal of Physical Chemistry A*, 2013, **87**, 649-653.
18. A. Amiri, R. Sadri, M. Shanbedi, G. Ahmadi, S. Kazi, B. Chew and M. N. M. Zubir, *Energy Conversion and Management*, 2015, **101**, 767-777.
19. S. J. Aravind, P. Baskar, T. T. Baby, R. K. Sabareesh, S. Das and S. Ramaprabhu, *The Journal of Physical Chemistry C*, 2011, **115**, 16737-16744.
20. H. Z. Zardini, M. Davarpanah, M. Shanbedi, A. Amiri, M. Maghrebi and L. Ebrahimi, *Journal of Biomedical Materials Research Part A*, 2014, **102**, 1774-1781.
21. H. Zare-Zardini, A. Amiri, M. Shanbedi, M. Memarpoor-Yazdi and A. Asoodeh, *Surface and Interface Analysis*, 2013, **45**, 751-755.
22. K. Miners, *Power Apparatus and Systems, IEEE Transactions on*, 1982, 751-756.
23. T. V. Oommen and E. M. Petrie, *Power Apparatus and Systems, IEEE Transactions on*, 1984, **PAS-103**, 1923-1931.
24. A. Amiri, M. Shanbedi, H. Eshghi, S. Z. Heris and M. Baniadam, *The Journal of Physical Chemistry C*, 2012, **116**, 3369-3375.
25. C. Choi, H. Yoo and J. Oh, *Current Applied Physics*, 2008, **8**, 710-712.
26. L. Chen, H. Xie, W. Yu and Y. Li, *Journal of Dispersion Science and Technology*, 2011, **32**, 550-554.
27. H. Ahmadi, A. Rashidi, A. Nouralishahi and S. S. Mohtasebi, *International Communications in Heat and Mass Transfer*, 2013, **46**, 142-147.
28. A. Amiri, M. Maghrebi, M. Baniadam and S. Zeinali Heris, *Applied Surface Science*, 2011, **257**, 10261-10266.
29. M. D. Ellison and P. J. Gasda, *The Journal of Physical Chemistry C*, 2008, **112**, 738-740.
30. J. L. Bahr and J. M. Tour, *Chemistry of Materials*, 2001, **13**, 3823-3824.
31. B. K. Price and J. M. Tour, *Journal of the American Chemical Society*, 2006, **128**, 12899-12904.
32. J. P. Holman, 1966.
33. M. Dong, L. Shen, H. Wang, H. Wang and J. Miao, *Journal of Nanomaterials*, 2013, **2013**, 164.
34. A. Amiri, M. Maghrebi, M. Baniadam and S. Z. Heris, *Applied Surface Science*, 2011, **257**, 10261-10266.
35. I. Kalinina, K. Worsley, C. Lugo, S. Mandal, E. Bekyarova and R. C. Haddon, *Chemistry of Materials*, 2011, **23**, 1246-1253.
36. DasA, PisanaS, ChakrabortyB, PiscanecS, S. K. Saha, U. V. Waghmare, K. S. Novoselov, H. R. Krishnamurthy, A. K. Geim, A. C. Ferrari and A. K. Sood, *Nat Nano*, 2008, **3**, 210-215.
37. B. Das, R. Voggu, C. S. Rout and C. N. R. Rao, *Chemical Communications*, 2008, DOI: 10.1039/B808955H, 5155-5157.
38. L. Feng, L. Yang, Z. Huang, J. Luo, M. Li, D. Wang and Y. Chen, *Scientific reports*, 2013, **3**.
39. R. Tian, X. Wang, M. Li, H. Hu, R. Chen, F. Liu, H. Zheng and L. Wan, *Applied Surface Science*, 2008, **255**, 3294-3299.

40. W. Lv, D.-M. Tang, Y.-B. He, C.-H. You, Z.-Q. Shi, X.-C. Chen, C.-M. Chen, P.-X. Hou, C. Liu and Q.-H. Yang, *ACS nano*, 2009, **3**, 3730-3736.
41. Y. Xie, Q. Huang, M. Liu, K. Wang, Q. Wan, F. Deng, L. Lu, X. Zhang and Y. Wei, *RSC Advances*, 2015, **5**, 68430-68438.
42. C.-F. Wang, S.-W. Kuo, C.-H. Lin, H.-G. Chen, C.-S. Liao and P.-R. Hung, *RSC Advances*, 2014, **4**, 36012-36016.
43. E. Moaseri, M. Maghrebi and M. Baniadam, *Materials & Design*, 2014, **55**, 644-652.
44. L. Vandsberger, McGill University, 2009.
45. B. White, S. Banerjee, S. O'Brien, N. J. Turro and I. P. Herman, *The Journal of Physical Chemistry C*, 2007, **111**, 13684-13690.
46. H. Wang, S. J. Ma, H. Yu, Q. Zhang, C. M. Guo and P. Wang, *Petroleum Science and Technology*, 2014, **32**, 2143-2150.
47. S. S. Park and N. J. Kim, *Journal of Industrial and Engineering Chemistry*, 2014, **20**, 1911-1915.
48. B. Pal, S. S. Mallick and B. Pal, *Journal of Industrial and Engineering Chemistry*, 2015, **25**, 99-104.
49. S. F. Seyed Shirazi, S. Gharehkhani, H. Yarmand, A. Badarudin, H. S. Cornelis Metselaar and S. N. Kazi, *Materials Letters*, 2015, **152**, 192-195.
50. S. S. J. Aravind, P. Baskar, T. T. Baby, R. K. Sabareesh, S. Das and S. Ramaprabhu, *The Journal of Physical Chemistry C*, 2011, **115**, 16737-16744.
51. N. Jha and S. Ramaprabhu, *The Journal of Physical Chemistry C*, 2008, **112**, 9315-9319.
52. L. S. Sundar, M. K. Singh, E. V. Ramana, B. Singh, J. Grácio and A. C. Sousa, *Scientific reports*, 2014, **4**.
53. S. Murshed, K. Leong and C. Yang, *Applied Thermal Engineering*, 2008, **28**, 2109-2125.
54. C.-J. Yu, A. Richter, A. Datta, M. Durbin and P. Dutta, *Physica B: Condensed Matter*, 2000, **283**, 27-31.
55. H. E. Patel, T. Sundararajan and S. K. Das, *Journal of Nanoparticle Research*, 2010, **12**, 1015-1031.
56. S. M. Ghiaasiaan, *Convective heat and mass transfer*, Cambridge University Press, 2011.
57. S. S. J. Aravind and S. Ramaprabhu, *RSC Advances*, 2013, **3**, 4199-4206.
58. M. Ikeda, T. Teranishi, M. Honda and T. Yanari, *Power Apparatus and Systems, IEEE Transactions on*, 1981, 921-928.
59. Y. Lv, Y. Zhou, C. Li, Q. Wang and B. Qi, *Electrical Insulation Magazine, IEEE*, 2014, **30**, 23-32.
60. M. A. Wahab, M. Hamada, A. Zeitoun and G. Ismail, *Electric Power Systems Research*, 1999, **51**, 61-70.
61. D. Kong, D. J. am Ende, S. J. Brenek and N. P. Weston, *Journal of Hazardous Materials*, 2003, **102**, 155-165.
62. G. H. Ko, K. Heo, K. Lee, D. S. Kim, C. Kim, Y. Sohn and M. Choi, *International Journal of Heat and Mass Transfer*, 2007, **50**, 4749-4753.
63. D. H. Fontes, G. Ribatski and E. P. Bandarra Filho, *Diamond and Related Materials*, 2015, **58**, 115-121.
64. M. Singh and L. Kundan, *Journal*, 2013.

Figure Caption:

Figure 1. Schematic of experimental transformer.

Figure 2. (a) FT-IR spectra, (b) Raman spectra, (c) thermogravimetric analysis (TGA) and Derivative thermogravimetric (DTG) curves of the pristine and MWNT-HA, (d-f) TEM images of MWNT-HA.

Figure 3. EDS spectra of Pristine MWNT and MWNT-HA.

Figure 4. (a) UV–Vis spectrum of MWNT-HA/TO coolant at different concentrations, (b) the colloidal stability of MWNT-HA in TO as a function of time and weight concentration and (c) the UV–Vis spectrum of the MWNT-HA for weight concentrations of 0.001 and 0.005 mechanically shaken 5 min every day.

Figure 5. Average particle size distribution after (a) 1 day, (b) 7 days, (c) 14 days, (d) 21 days, (e) 28 days, (f) 35 days and (g) 1 day.

Figure 6. (a) Electrical conductivity and (b) electrical resistivity of MWNT-HA/TO coolant at different weight concentration and temperatures.

Figure 7. Thermal conductivity plot of pure TO and MWNT-HA/TO coolant at different weight concentrations.

Figure 8. (a) Natural convection heat transfer coefficient, (b) Nusselt number (Natural), (c) forced convection heat transfer coefficient and (d) Nusselt number (forced) of pure TO and MWNT-HA/TO coolant.

Figure 9. The dielectric breakdown voltage of pure oil (a) with and (b) without 30 min sonication (c) MWNT-HA/TO at (c) 0.001 and (d) 0.005.

Figure 10. Density of the MWNT-HA/TO coolants at different concentrations and temperatures.

Figure 11. Flash point of pure TO and MWNT-HA/TO coolants

Figure 12. (a) The viscosity of pure TO and MWNT-HA/TO coolants at different weight concentrations and temperatures at shear rate of 235 S^{-1}, (b) viscosity enhancement MWNT-HA/TO coolants at different weight concentrations in comparison with pure TO.

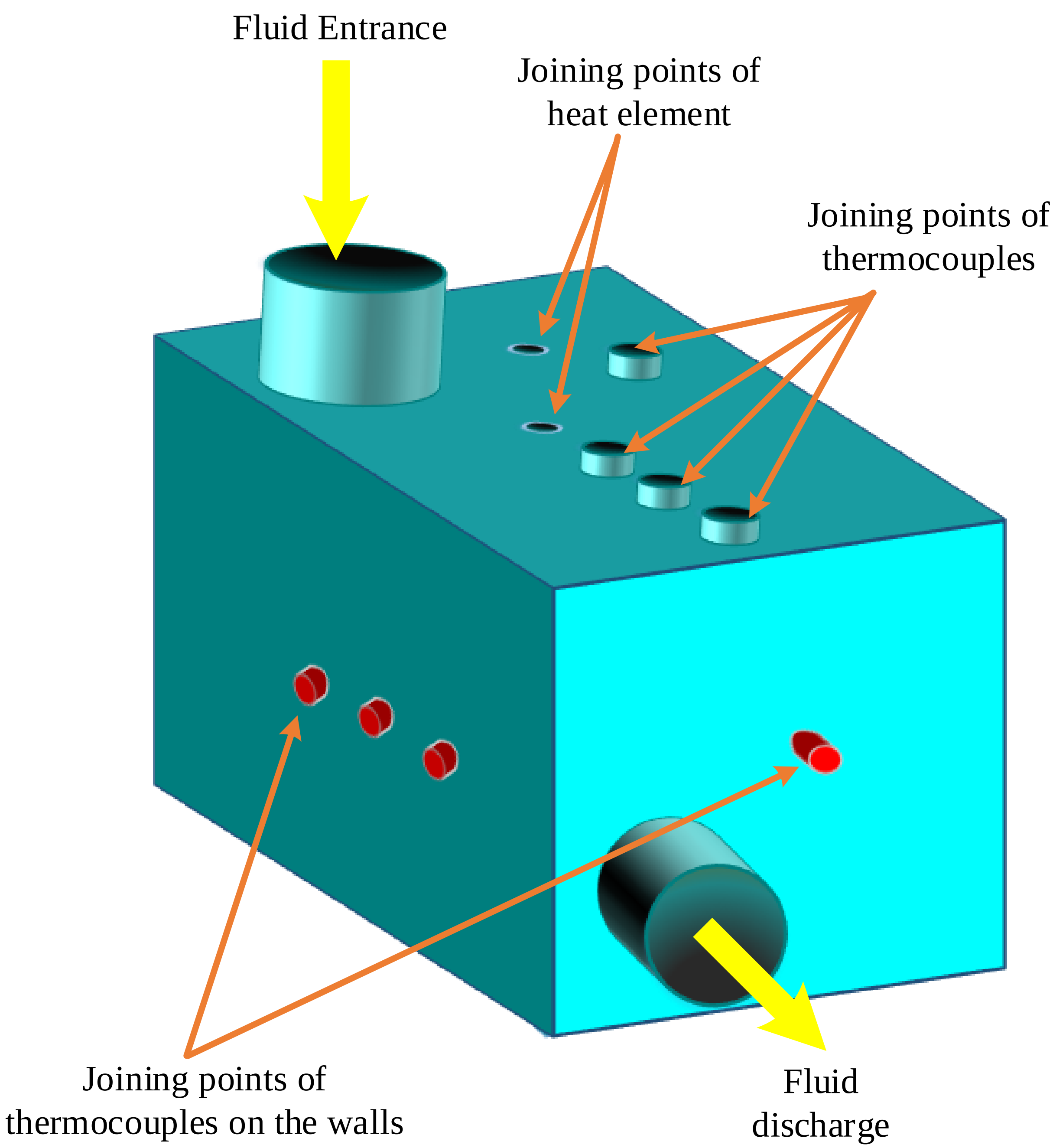
Fluid Entrance
Joining points of
heat element
Joining points of
thermocouples
Joining points of
thermocouples on the walls
Fluid
discharge

Figure 1

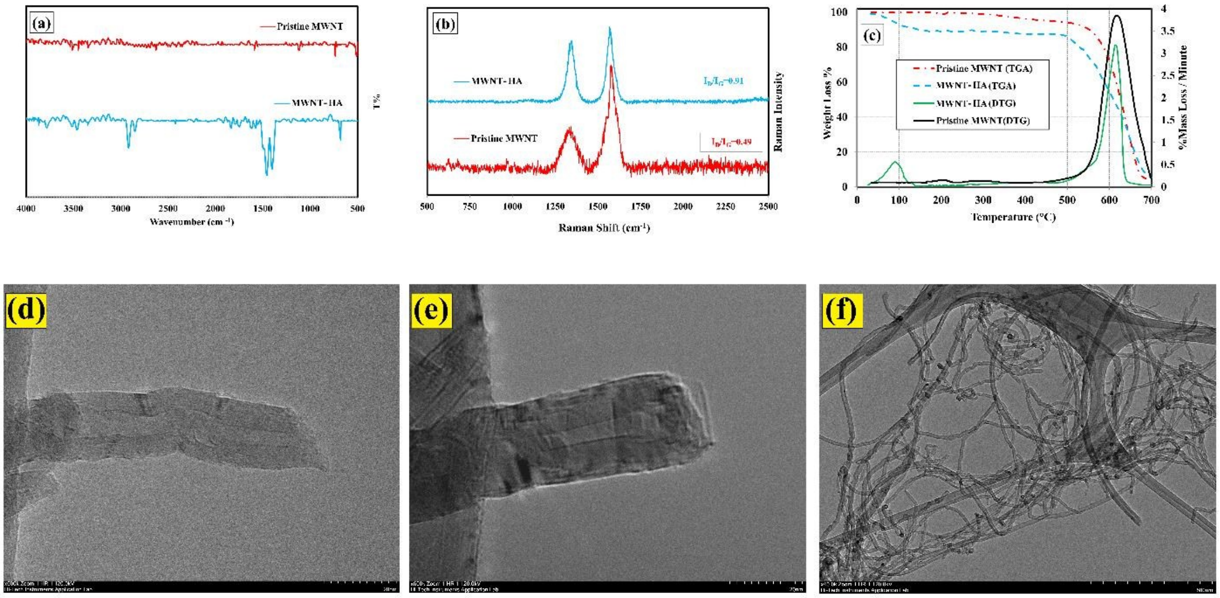
(a)
Pristine MWNT
MWNT-HA
T%
Wavenumber (cm⁻¹)
(b)
MWNT-HA
Pristine MWNT
Raman Intensity
Raman Shift (cm⁻¹)
(c)
Pristine MWNT (TGA)
MWNT-HA (TGA)
MWNT-HA (DTG)
Pristine MWNT(DTG)
Weight Loss %
%Mass Loss / Minute
Temperature (°C)
(d)
(e)
(f)

Figure 2.

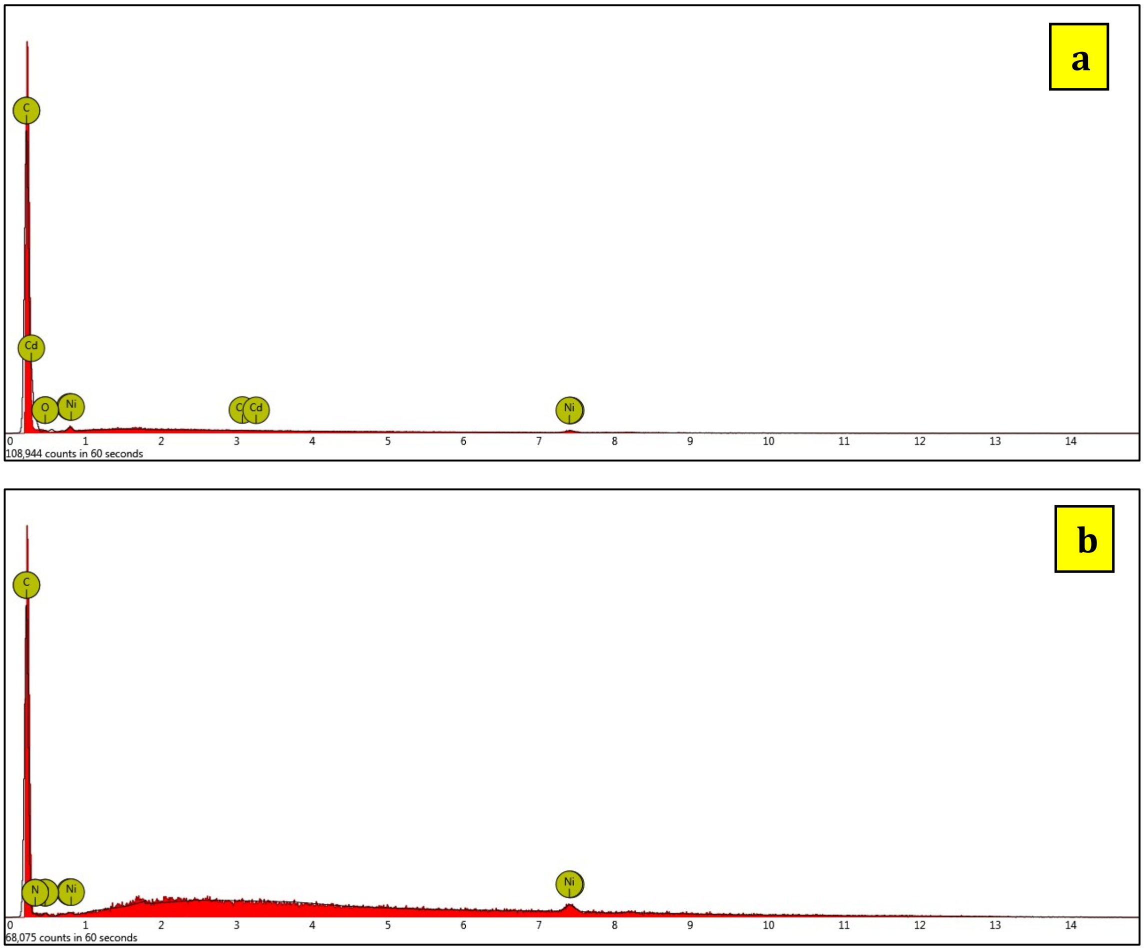
a
C
Cd
O
Ni
C
Cd
Ni
0 1 2 3 4 5 6 7 8 9 10 11 12 13 14
108,944 counts in 60 seconds
b
C
N
Ni
Ni
0 1 2 3 4 5 6 7 8 9 10 11 12 13 14
68,075 counts in 60 seconds

Figure 3.

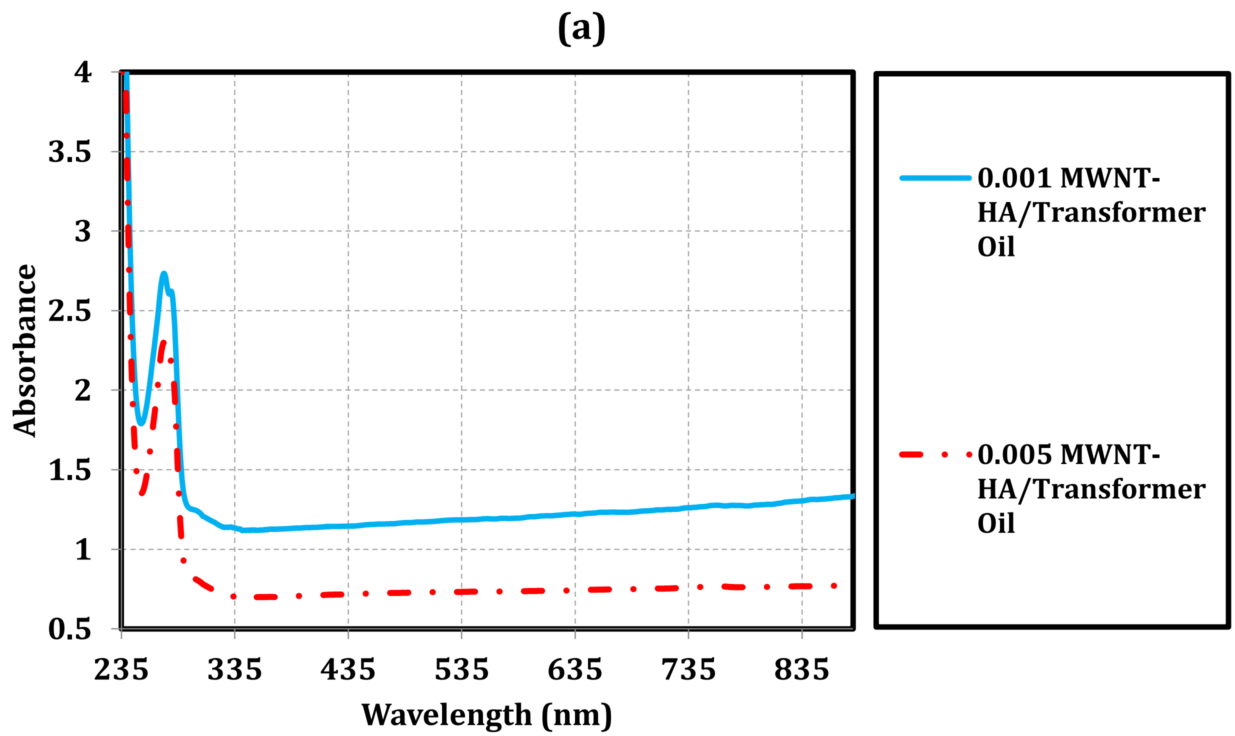
(a)
4
3.5
3
2.5
2
1.5
1
0.5
Absorbance
235
335
435
535
635
735
835
Wavelength (nm)
0.001 MWNT-HA/Transformer Oil
0.005 MWNT-HA/Transformer Oil

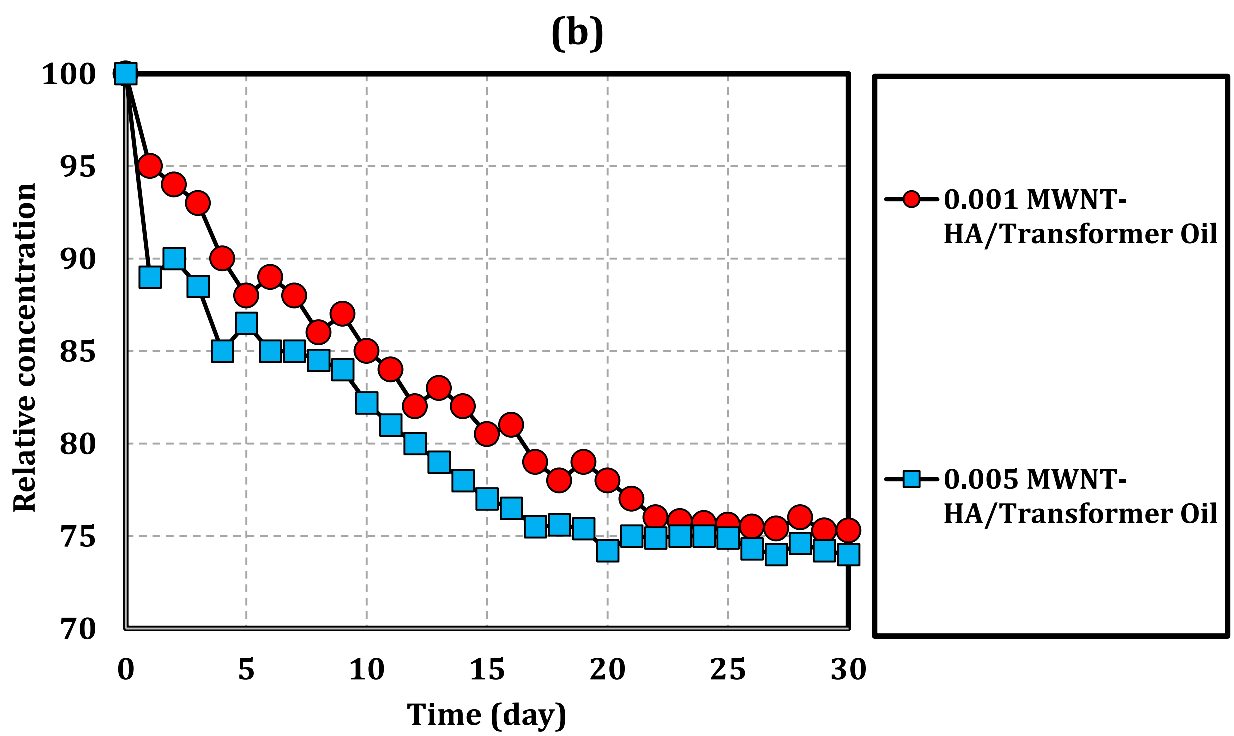
(b)
100
95
90
85
80
75
70
Relative concentration
0
5
10
15
20
25
30
Time (day)
0.001 MWNT-HA/Transformer Oil
0.005 MWNT-HA/Transformer Oil

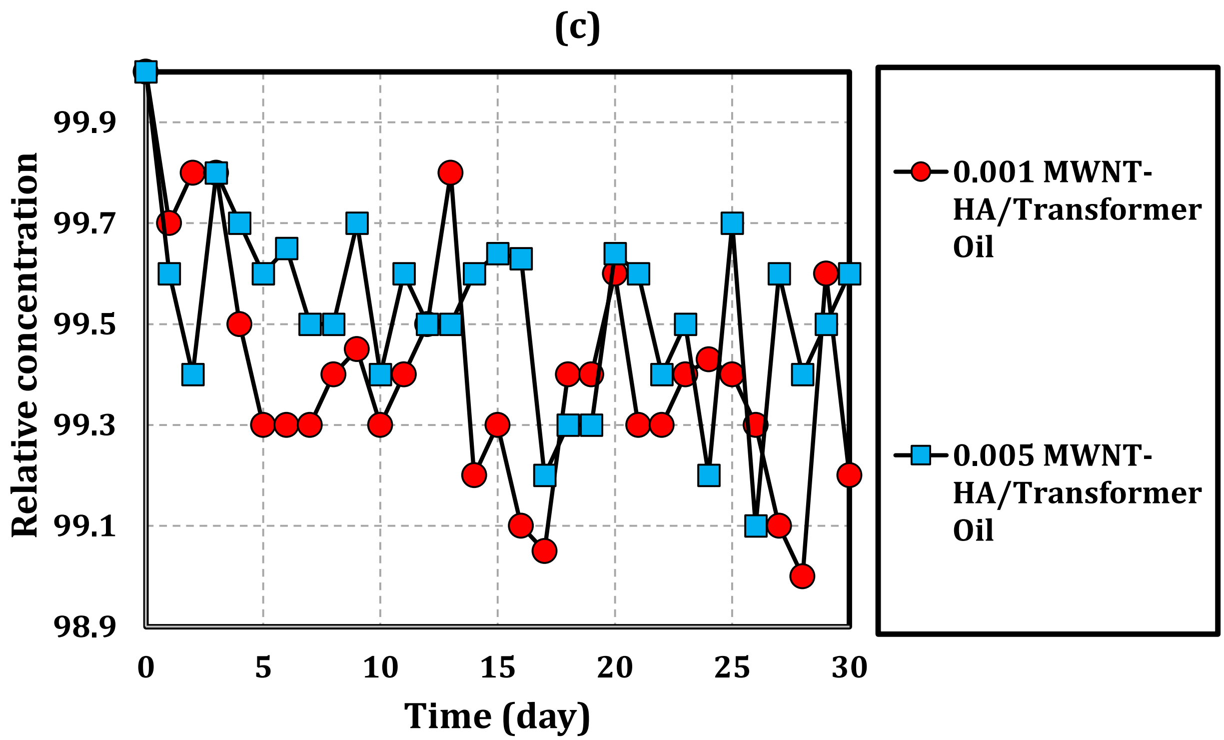
(c)
Relative concentration
99.9
99.7
99.5
99.3
99.1
98.9
0
5
10
15
20
25
30
Time (day)
0.001 MWNT-HA/Transformer Oil
0.005 MWNT-HA/Transformer Oil

Figure 4

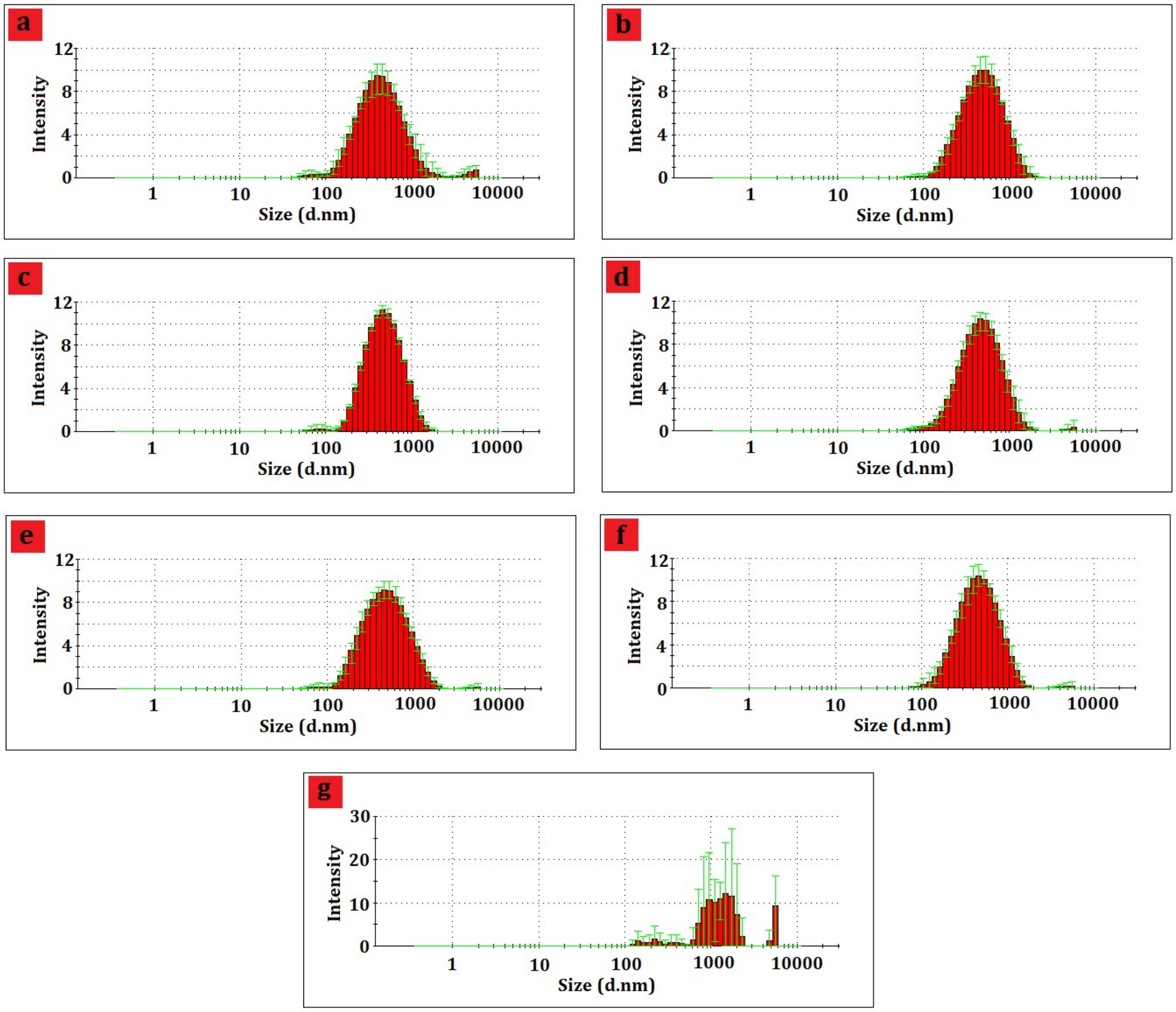

Figure 5.

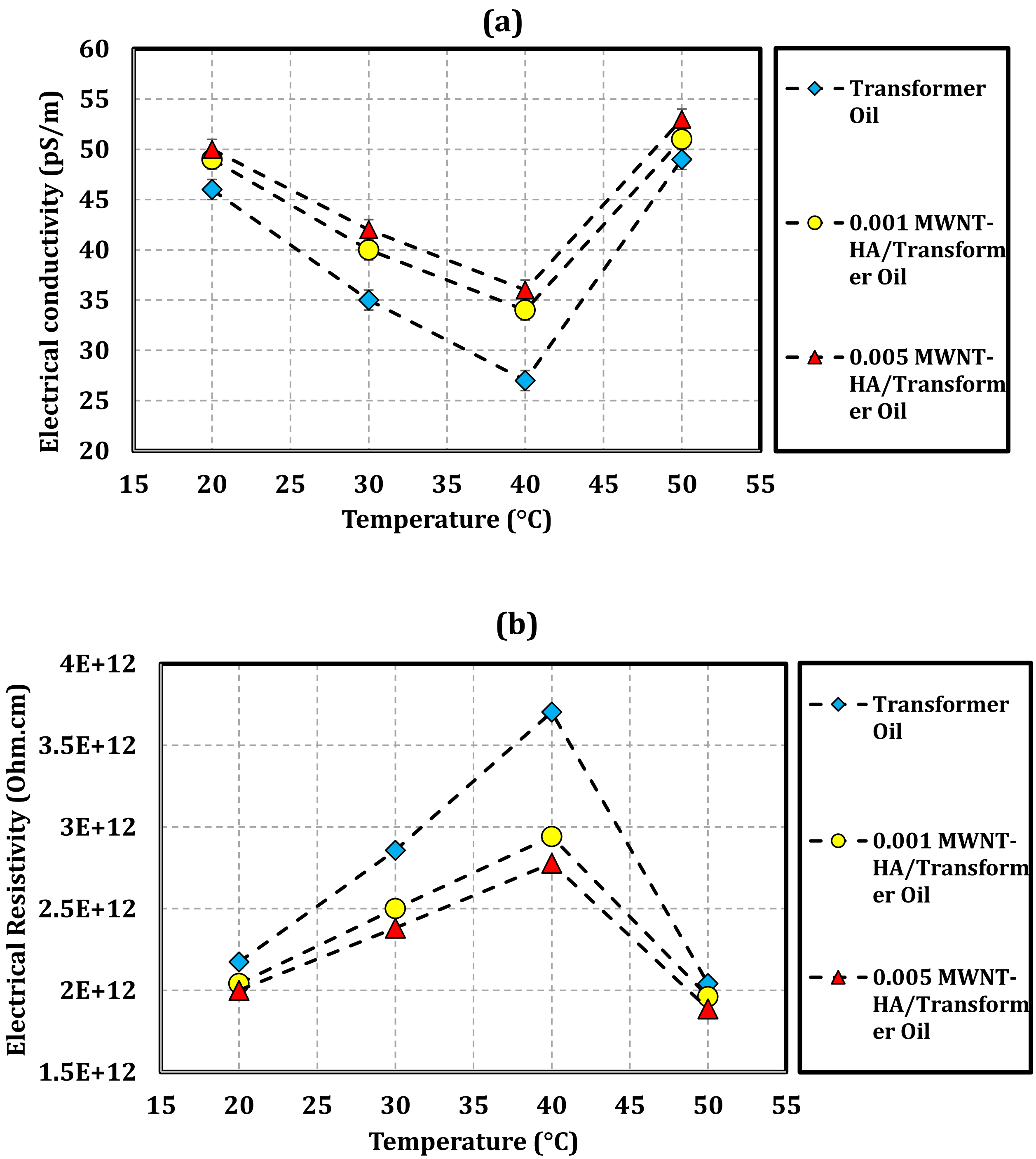
(a)
Electrical conductivity (pS/m)
60
55
50
45
40
35
30
25
20
15
20
25
30
35
40
45
50
55
Temperature (°C)
Transformer Oil
0.001 MWNT-HA/Transformer Oil
0.005 MWNT-HA/Transformer Oil
(b)
Electrical Resistivity (Ohm.cm)
4E+12
3.5E+12
3E+12
2.5E+12
2E+12
1.5E+12
15
20
25
30
35
40
45
50
55
Temperature (°C)
Transformer Oil
0.001 MWNT-HA/Transformer Oil
0.005 MWNT-HA/Transformer Oil

Figure 6.

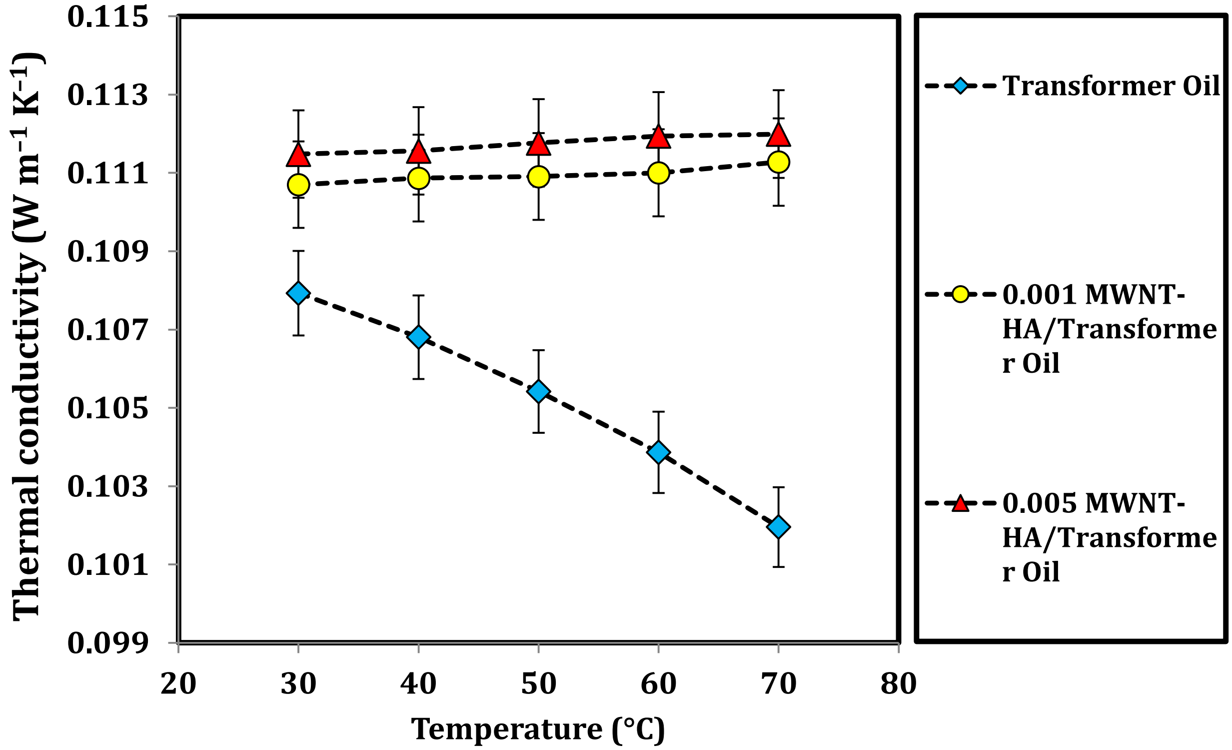
0.115
0.113
0.111
0.109
0.107
0.105
0.103
0.101
0.099
Thermal conductivity (W m-1 K-1)
20
30
40
50
60
70
80
Temperature (°C)
Transformer Oil
0.001 MWNT-HA/Transformer Oil
0.005 MWNT-HA/Transformer Oil

Figure 7.

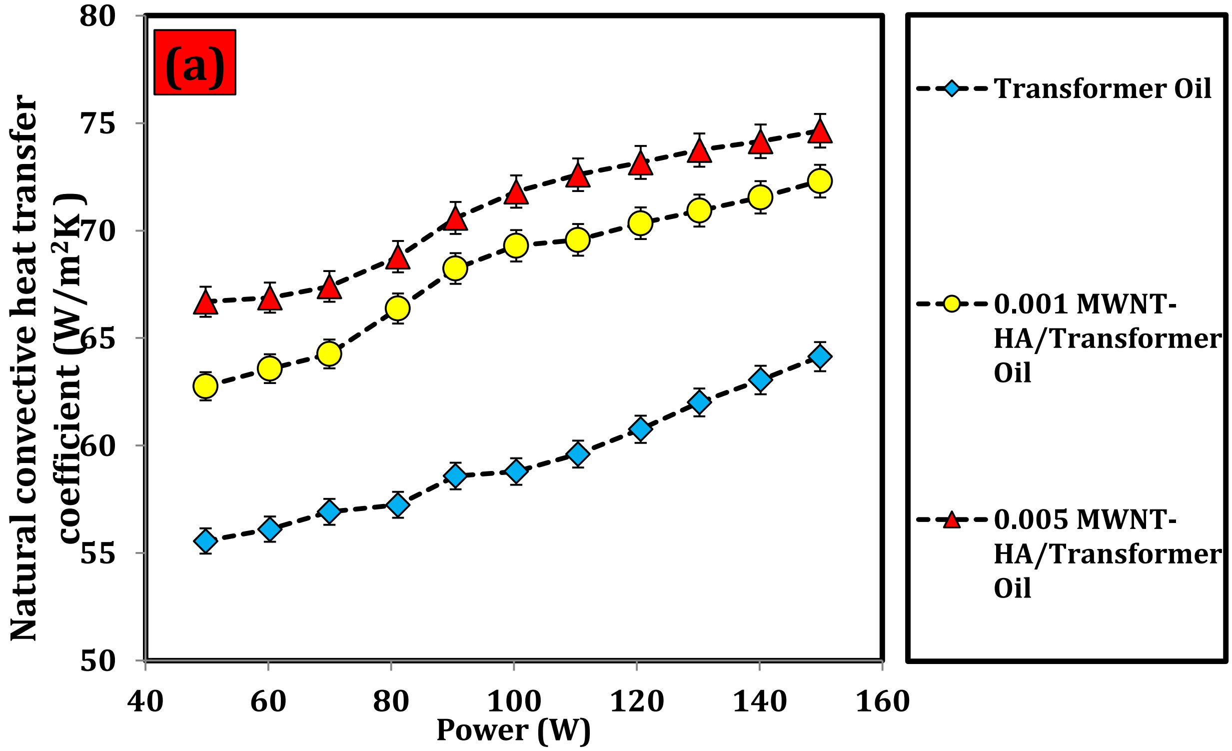
(a)
Natural convective heat transfer coefficient (W/m²K)
80
75
70
65
60
55
50
40
60
80
100
120
140
160
Power (W)
Transformer Oil
0.001 MWNT-HA/Transformer Oil
0.005 MWNT-HA/Transformer Oil

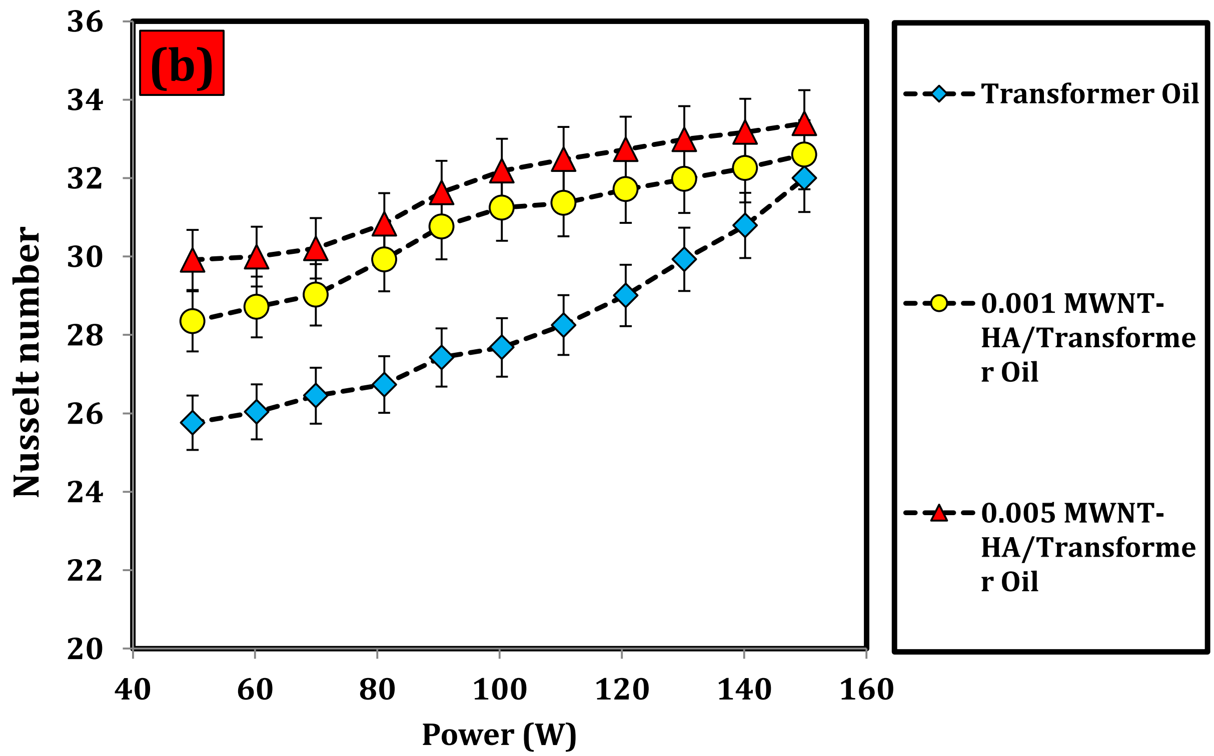
(b)
Nusselt number
36
34
32
30
28
26
24
22
20
40
60
80
100
120
140
160
Power (W)
Transformer Oil
0.001 MWNT-HA/Transforme r Oil
0.005 MWNT-HA/Transforme r Oil

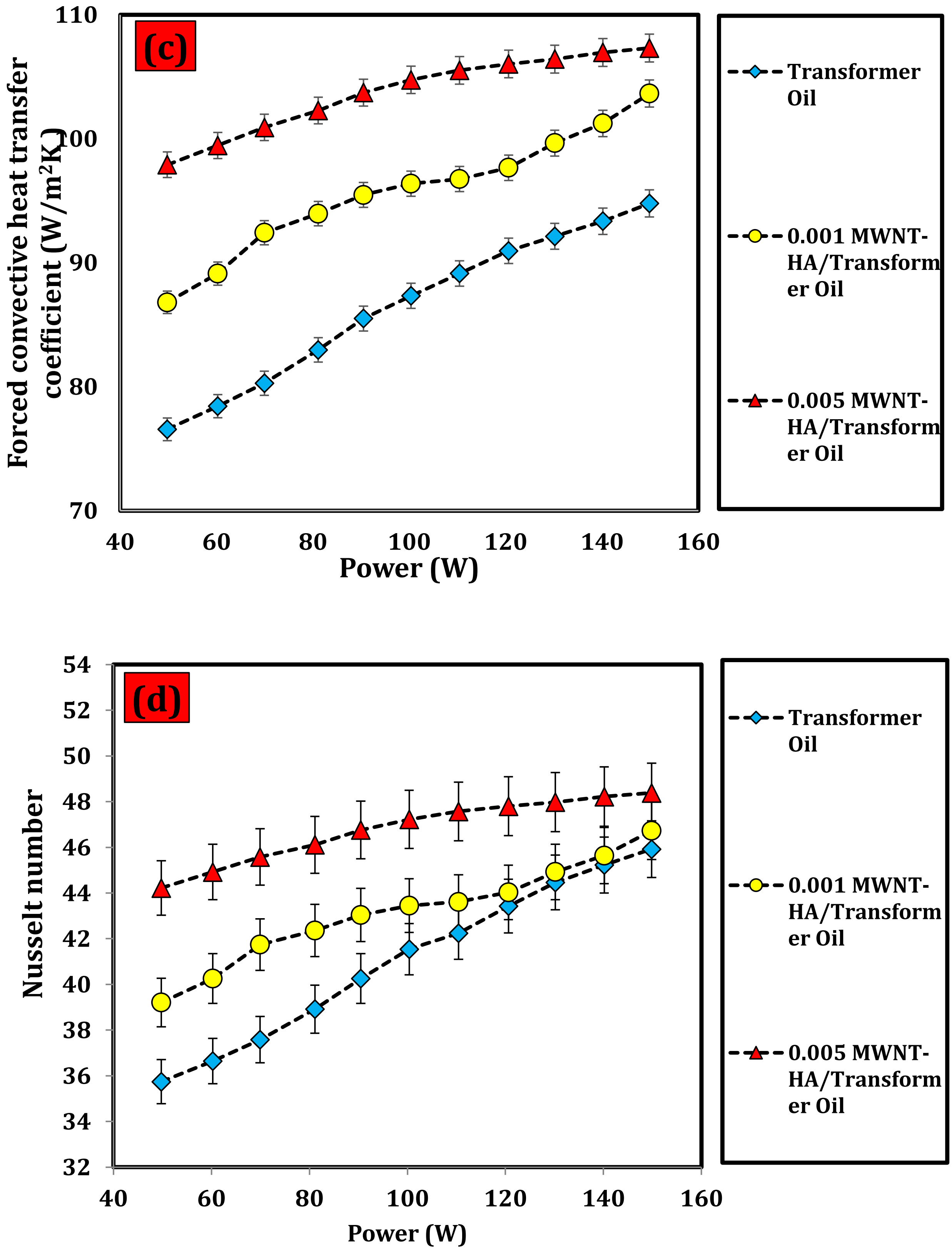
(c)
110
100
90
80
70
Forced convective heat transfer coefficient (W/m^{2}K)
40
60
80
100
120
140
160
Power (W)
Transformer Oil
0.001 MWNT-HA/Transformer Oil
0.005 MWNT-HA/Transformer Oil
(d)
54
52
50
48
46
44
42
40
38
36
34
32
Nusselt number
Power (W)
Transformer Oil
0.001 MWNT-HA/Transformer Oil
0.005 MWNT-HA/Transformer Oil

Figure 8.

(a)

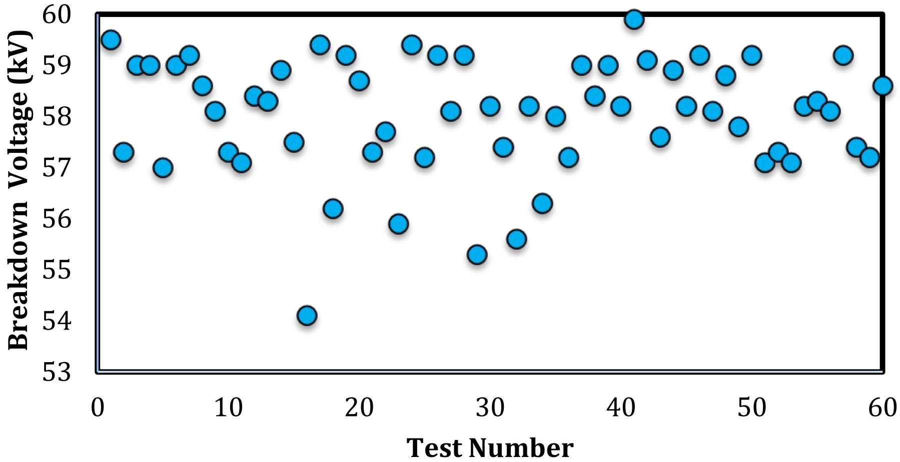
Breakdown Voltage (kV)
60
59
58
57
56
55
54
53
0
10
20
30
40
50
60
Test Number

(b)

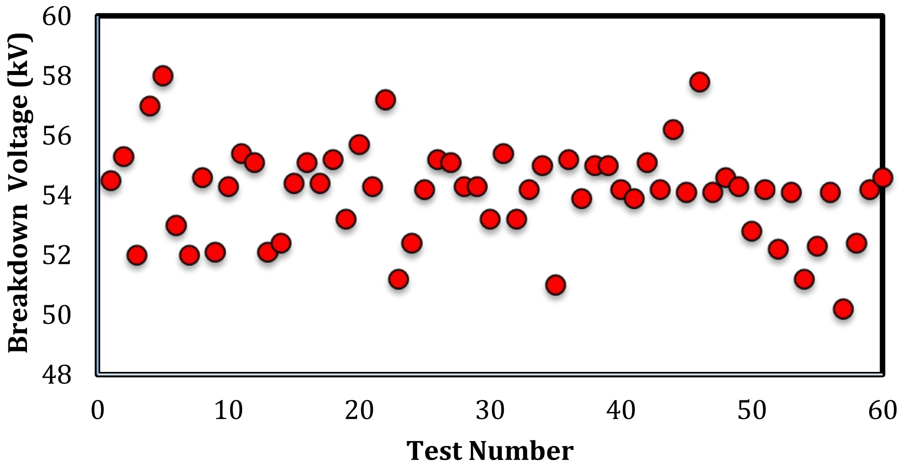
Breakdown Voltage (kV)
60
58
56
54
52
50
48
0
10
20
30
40
50
60
Test Number

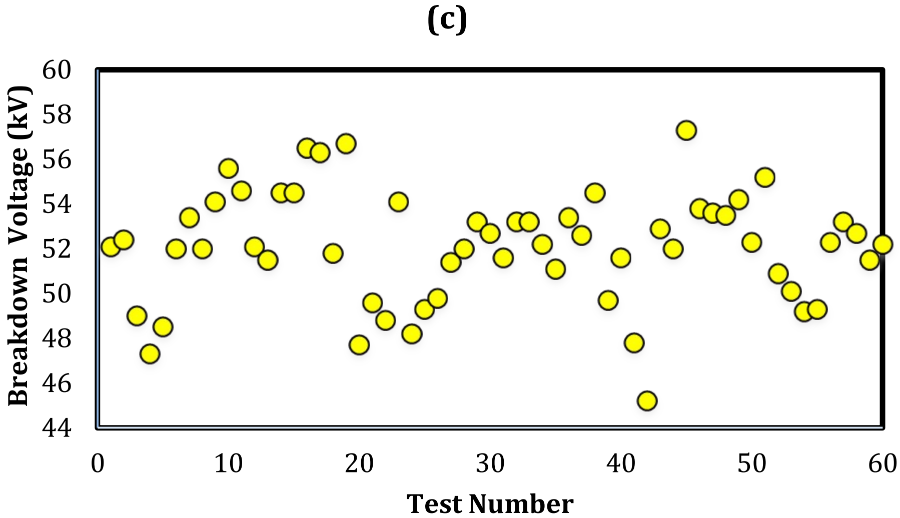
(c)
Breakdown Voltage (kV)
60
58
56
54
52
50
48
46
44
0
10
20
30
40
50
60
Test Number

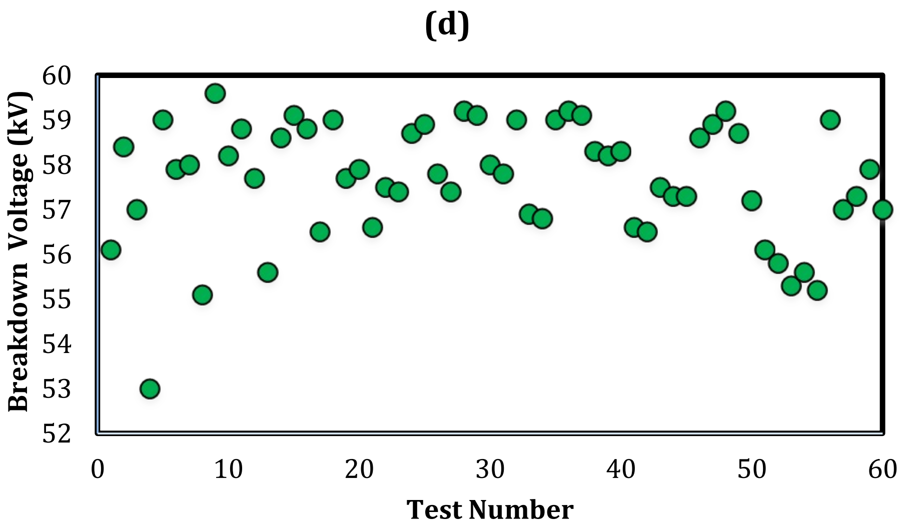
(d)
Breakdown Voltage (kV)
60
59
58
57
56
55
54
53
52
0
10
20
30
40
50
60
Test Number

Figure 9.

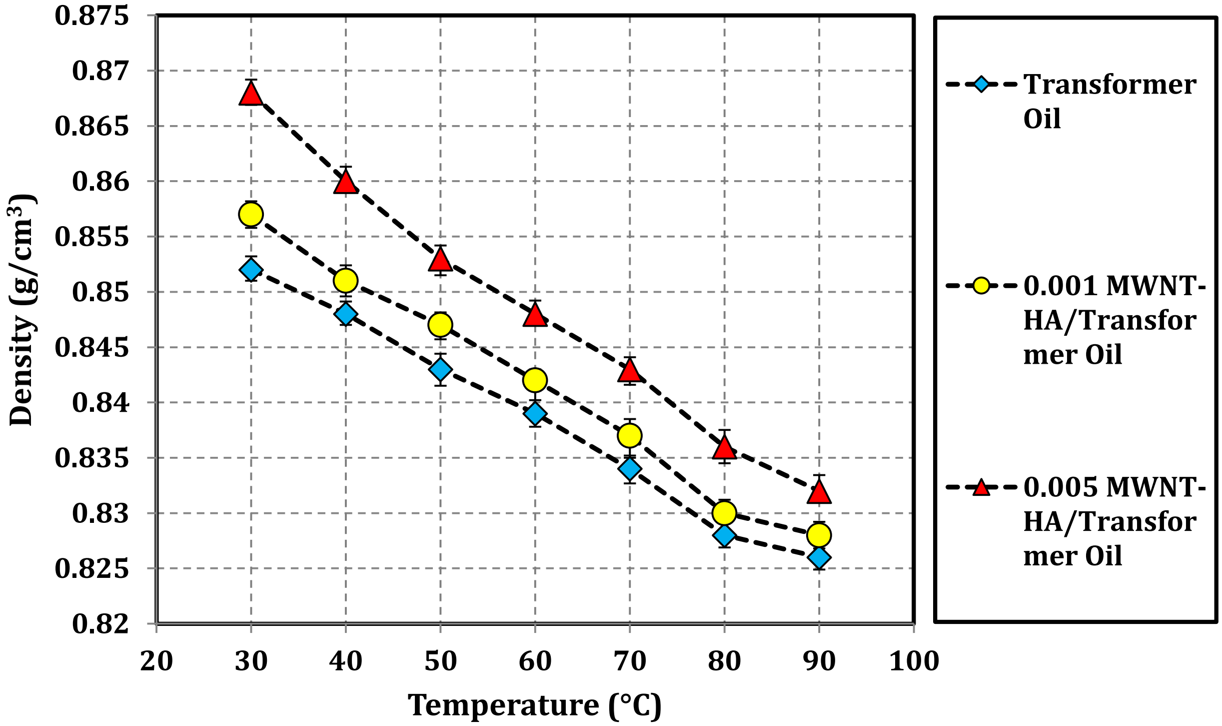
0.875
0.87
0.865
0.86
0.855
0.85
0.845
0.84
0.835
0.83
0.825
0.82
Density (g/cm³)
20
30
40
50
60
70
80
90
100
Temperature (°C)
Transformer Oil
0.001 MWNT-HA/Transformer Oil
0.005 MWNT-HA/Transformer Oil

Figure 10.

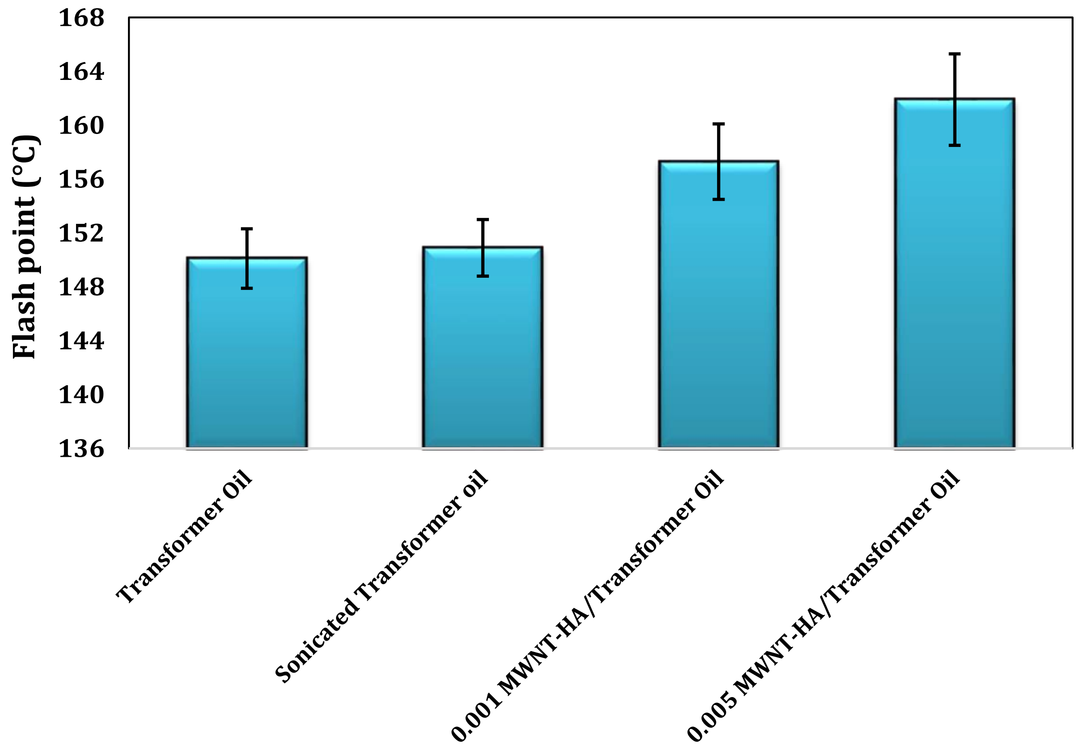
168
164
160
156
152
148
144
140
136
Flash point (°C)
Transformer Oil
Sonicated Transformer oil
0.001 MWNT-HA/Transformer Oil
0.005 MWNT-HA/Transformer Oil

Figure 11.

(a)

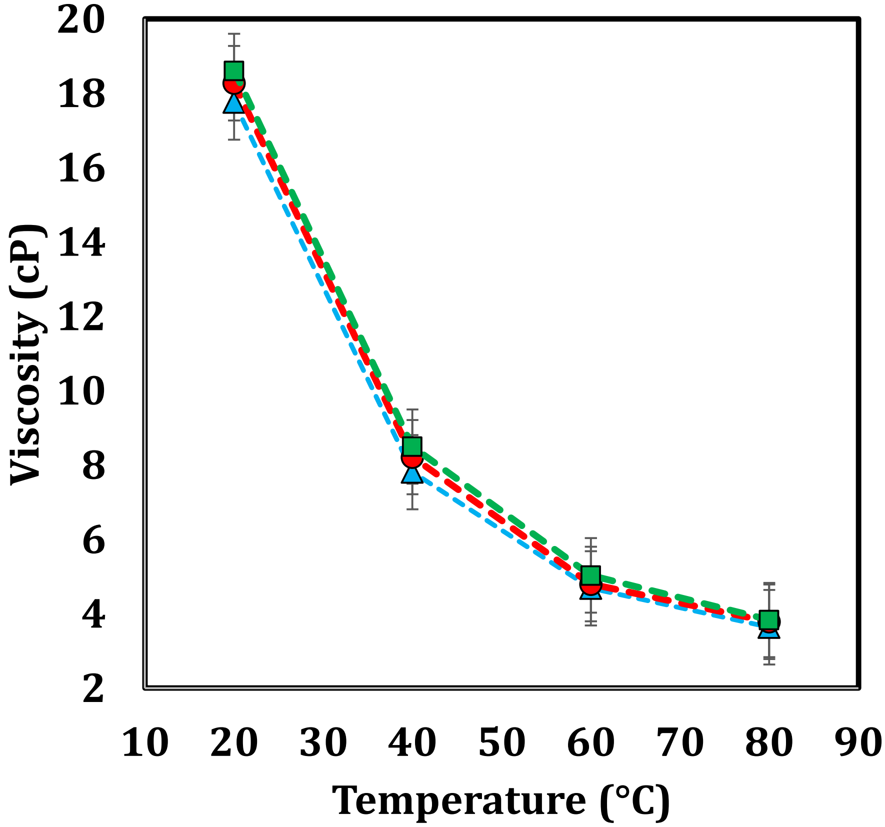

Viscosity (cP)
20
18
16
14
12
10
8
6
4
2
10
20
30
40
50
60
70
80
90
Temperature (°C)

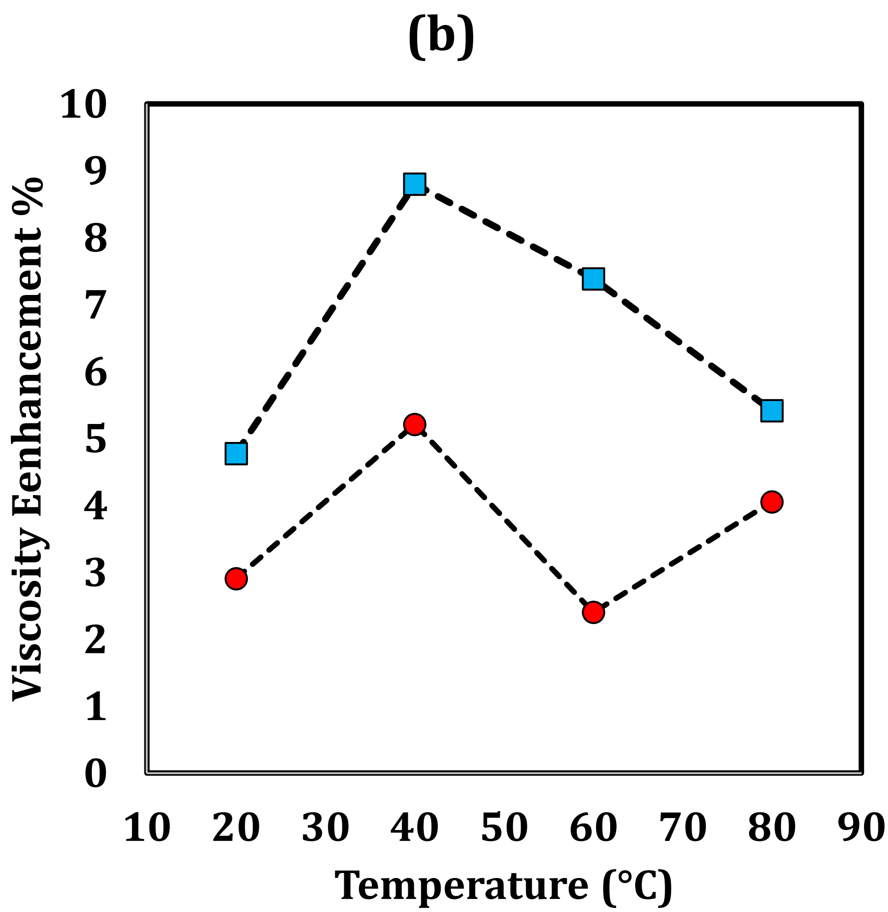
(b)
Viscosity Eenhancement %
0
1
2
3
4
5
6
7
8
9
10
10
20
30
40
50
60
70
80
90
Temperature (°C)

Figure 12

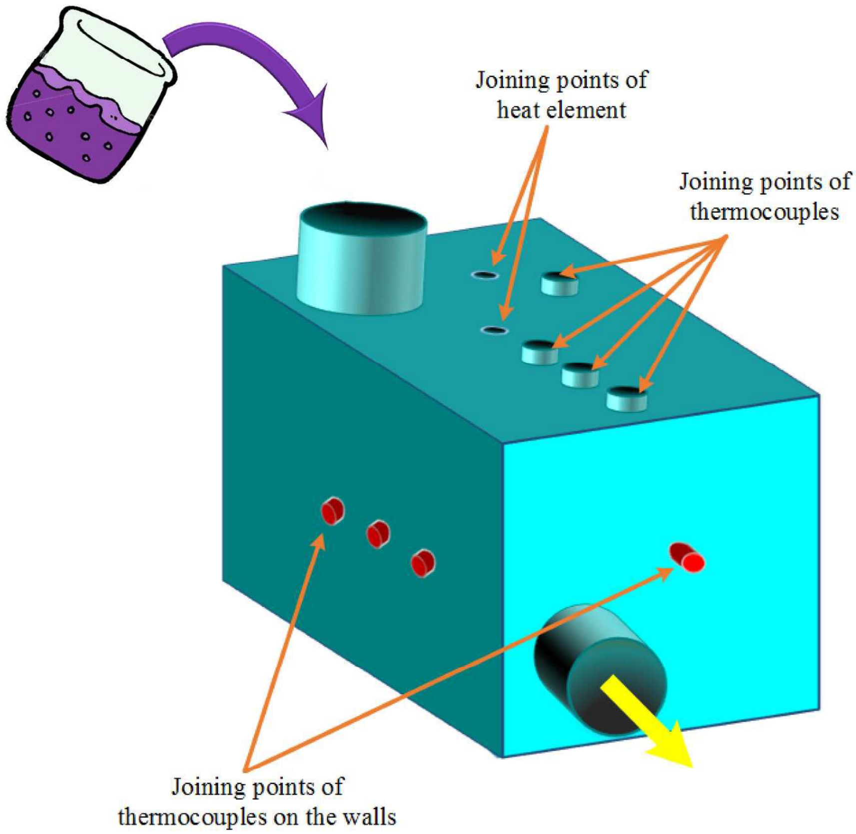

1105x1005mm (96 x 96 DPI)